Pessimistic Hazmat Network Design Problem with Emergency Team Location Considering Uncertain Response Time

by

Jeremy Briere

A thesis
presented to the University of Waterloo
in fulfillment of the
thesis requirement for the degree of
Master of Applied Science
in
Management Sciences

Waterloo, Ontario, Canada, 2021

Author's Declaration

I hereby declare that I am the sole author of this thesis. This is a true copy of the thesis, including any required final revisions, as accepted by my examiners.

I understand that my thesis may be made electronically available to the public.

Abstract

Focusing on a road network where hazmat shipments need to be transported from the origins to destinations, this thesis proposes a pessimistic approach to mitigate the risk associated with the transportation of hazardous materials (hazmat). More specifically, two stakeholders are involved in the process, the government entity implementing risk mitigation mechanisms to minimize the maximum network risk, and the hazmat carriers fulfilling hazmat demand to minimize their total travel distance. Due to the conflicting interests and decision process of the two parties, a bilevel model structure is used, and the pessimistic perspective is assumed to ensure that the carriers' worst behavior can be avoided.

The risk mitigation mechanisms implemented in this work include 1) network design, where certain road segments (i.e., links/arcs) are made unavailable to hazmat shipments, and 2) locating emergency response teams to attend to possible incidents in a timely manner. The uncertain nature of the response time is incorporated through the chance constraints for both the most and least desired response times, reflecting the satisfaction levels of emergency services.

Because of the complexity of the bilevel model, we investigate two solution methods. The first one is to reformulate the problem into a single level model that is linearized later. The second one is a heuristic algorithm that breaks the problem into two stages that can be solved sequentially. We then present experimental results based on a transportation network in China, showing the efficacy of the model in a real-life scenario and providing insights regarding the nature of the solutions.

Acknowledgements

I would like to thank my supervisors, Prof. James H Bookbinder and Prof. Ginger Ke, who introduced me to the topic of hazmat transportation, and helped me greatly through the research process.

Additionally, I would like to express my gratitude to my family who have supported me throughout my education.

Table of Contents

List of Figures viii

List of Tables ix

Acronyms xi

1 Introduction 1

2 Literature Review 4

2.1 Hazmat Risk 4

2.2 Hazmat Emergency Response 10

2.3 Hazmat Transportation Network Design (HTND) 13

2.4 Pessimistic Bilevel Models 15

2.4.1 Bilevel Models 15

2.4.2 Pessimistic Formulation 17

2.5 Literature Gaps and Positioning of the Present Work 20

3 Model 23

3.1 Problem Definition 23

3.1.1 Risk Measurement 24
3.1.2 Emergency Response 25
3.2 A Pessimistic Bilevel Model Structure 29
3.3 Assumptions 32
3.4 Notation 33
3.5 Mathematical Formulation 34
3.5.1 Upper-Level 34
3.5.2 Lower-Level 35
3.6 Higher Connectivity Model 36

4 Solution Methodologies **38**
4.1 Single-Level Reformulation 38
4.1.1 Duality 39
4.1.2 Single-level Formulation 40
4.2 A Two-Stage Heuristic Algorithm 43
4.2.1 Algorithm 44
4.3 Computational Results 48

5 Case Study **54**
5.1 Network Structure and Data Estimation 54
5.1.1 Distance 55
5.1.2 Risk 56
5.1.3 Time 57
5.1.4 Response Time Factor (RTF) 58
5.1.5 Other data 59

5.2 Algorithm Performance 60
5.3 Performance Comparison of MCV and MCN 62
5.4 Comparison of Risk Pessimism and Risk Equity 71
5.5 Comparison of Risk Mitigation Mechanisms 73
5.6 Sensitivity Analyses 75
5.6.1 T_{best}, T_{worst} 75
5.6.2 Emergency Service Satisfaction Rates (β, γ) 77
5.6.3 Variance of Response Time (η) 78
5.6.4 Response Time Factor (RTF) Percentile 78

6 Conclusion and Future Research **80**

References **83**

Appendices **90**

A Bilevel Model **91**

B Single Level Problem Linearization **93**

C Improved Linear Model **95**

List of Figures

3.1 Arc Coverage 26

3.2 Bilevel Structure of Problem 29

3.3 A simple example 31

5.1 Nanchang Network (Ke et al., 2020) 55

5.2 Distribution of Risk of Nanchang Network 57

5.3 Normalized CPU per shipment 62

5.4 MCV: HRT locations and available road links (5 HRTs) 64

5.5 MCN: HRT locations and available road links (5 HRTs) 65

5.6 Risk distribution (5 HRTs) 66

5.7 Shipment 4 route comparison (5 HRTs) 67

5.8 Shipment 4 route comparison (7 HRTs) 68

5.9 HRT locations and available road links (3 HRTs) 69

5.10 Comparison of Approaches 71

5.11 Trade-off between θ and μ 73

5.12 HRT locations and available road links for HTND and HRTO 75

List of Tables

2.1 A Comparison Between Taslimi et al. (2017) and the Present Research . . 21

3.1 Cost/Risk with HRT 31

4.1 Problem Size Comparison of SLP & SLPIL 42
4.2 Problem Size Comparison of SLP & SLPIL - Example 42
4.3 Problem Size Comparison of SLPIL & Heuristic Algorithm 48
4.4 Problem Size Comparison of SLPIL & Heuristic Algorithm - Example . . . 48
4.5 Solution Comparison of SLP and SLPIL 50
4.6 Solution Comparison of SLPIL and HM 52

5.1 Hazmat Types, $k \in \mathcal{K}$ 56
5.2 Response Time Factor, adapted from the Transportation Research Board and National Academies of Sciences, Engineering, and Medicine (2011) . . 59
5.3 Summary of Base Parameters 60
5.4 Sample Shipment Set 60
5.5 SLPIL Basic Performance on Nanchang Network 61
5.6 Comparison of Results: MCV & MCN (5 HRTs) 63
5.7 Comparison of Results: MCV & MCN (7 HRTs) 68

5.8 Comparison of Results: MCV & MCN (3 HRTs) 69
5.9 Comparison of Results: MCV & MCN (30 shipments, 5 HRTs) 70
5.10 Trade-off: MCV 72
5.11 Trade-off: MCN 72
5.12 Risk Mitigation Mechanisms Comparison 74
5.13 Sensitivity Analysis - Summary of Parameters 76
5.14 Sensitivity Analysis: Response Time 76
5.15 Sensitivity Analysis: γ, β 77
5.16 Sensitivity Analysis: Response Time Variance 78
5.17 Sensitivity Analysis: Response Time Factor (RTF) Percentile 79

Acronyms

HRT Hazmat Response Team. viii–x, 3, 11, 12, 15, 20, 21, 25–27, 29–37, 42–46, 53, 58, 60, 64–70, 73, 74, 76, 80, 81

HTND Hazmat Transportation Network Design. 13, 43, 45

KKT Karush–Kuhn–Tucker. 14, 16, 39

RTF Response Time Factor. vi, vii, ix, x, 10, 11, 21, 28, 37, 46, 58, 59, 76–79

US DOT US Department of Transportation. 4

US FMCSA US Federal Motor Carrier Safety Administration. 1, 4, 83

US PHMSA US Pipeline and Hazardous Materials Safety Administration. 1, 4, 83

Chapter 1

Introduction

Hazardous materials, commonly referred to as *hazmat*, can be defined as "materials posing an unreasonable threat to the public and the environment" and are categorized according to nine categories: explosives, gases, flammable liquids and solids, oxidizing substances, poisonous and infectious substances, radioactive materials, corrosive, and dangerous goods (US FMCSA, 2019). Taking part in most industries, these materials therefore need to be transported from their origin, where they are sourced, to their destination, location of their usage. Most common transportation modes include road (highway), air, railway, and water. Because of the harmful nature of these goods, the transportation of hazmat is very risky as an accident may result in substantial damages to the surrounding areas, including the population and environment. During the 2011-2020 period, there were a total of 176,127 hazmat-related accidents, of which 156,323 happened on the highway, resulting in a total of 1,806 injuries and ∼$900M in damages (US PHMSA, 2021). Reducing the likelihood of accidents happening, as well as diminishing their impact, represents an important step towards decreasing the number of incidents and the consequences caused.

A number of different approaches can be taken towards reducing risk, generally through policies implemented by the governing body (government) to influence the behavior of the users of the transportation network (carriers), with the goal of diminishing the risk according to specific goals. By doing so, the parties involved have diverging objectives and act in their best interests, where the government needs to take into account the hazmat

carriers' decisions (usually minimize shipping costs or travel distances) and the carriers have to abide by the regulation imposed. This relationship can be described by a bilevel model, with the government in the upper-level and the carriers in the lower one (Erkut et al., 2007).

Two main policies have been adopted over the years to control the risk imposed on the network and its surrounding area: Hazmat Transportation Network Design (HTND) and Toll Setting (TS). The first one refers to the problem of deciding which network arcs to make available or limit their use for the transportation of hazmat, whereas the latter relates to the idea of placing tolls on road segments. Both of these approaches affect the risk caused by the carriers' hazmat shipments, as they directly affect their objective. HTND, first introduced by Kara and Verter (2004), can be seen as a more restrictive method, as it forbids the use of network links. But existing research has shown its effectiveness in significantly reduce the network risk associated with hazmat transportation.

The previous studies in HTND assumed an optimistic perspective, where the carriers always choose the shortest paths that most preferred by the government, i.e., with the lowest risks. This assumption may not be true as the carriers may choose to take an alternative path with higher risk especially when more than one paths with the same distance exist. Hence, it is logical for the government to avoid the worst-case scenario where the carriers' choice is not preferred. This is referred to as a pessimistic point of view. To account for this, a more resilient min-max expression is developed.

The main idea of HTND is to induce the carriers to avoid highly risky (large population density and/or high incident rate) road paths for hazmat. However, once an incident occurs, the consequence can be catastrophic, even in a less risky area. Therefore, on top of regulating the road network, constructing a responsive emergency system become extremely necessary. The majority of emergency literature applied covering models to maximize the number of demand nodes in the system with minimum number of facilities. This type of models can be over simplified given the crisp cut between "fully covered" and "not covered at all", while, in a real-world situation, the responsiveness of an emergency system is directly related to the response time to any incidents. We, herein, integrated the time aspect to the assessment of arc coverage. Rather than a simple judgement of covered or not covered, the degree of coverage is determined by comparing the response

time from an Hazmat Response Team (HRT) to an incident location (network arc/link) with two thresholds, respectively the most and least desired response time. Moreover, the response time is uncertain by nature, due to a number of factors, such as traffic congestion, road condition, severe weather, to name a few. The model we develop adopts the chance constraints for uncertain response time to further enhance the risk minimization.

Taking the above considerations into account, we propose a model that minimizes the maximum network risk through a pessimistic bilevel approach. We combine a passive mechanism, through HTND, and an active mechanism, through emergency coverage, to build a hazmat network that reduces risk by opening and closing some road segments, as well as providing emergency services in an optimal manner by locating hazmat response teams accordingly. Two bilevel models are developed, one aiming for coverage guarantee, and the other for connectivity ensuring. Because of the bilevel structure of the model and its complexity, we study different solution methodologies, an exact one and a heuristic algorithm, which are benchmarked against each other to show the time/accuracy trade-off. To better understand the practicality of the models and algorithm, a real transportation network in China is analyzed as a case study. We analyze the resulting base case and perform sensitivity analysis around the main parameters. Additionally, we compare the pessimistic solution to a risk equity model, showing that one hinders the other. The benefits of different risk mitigation mechanisms are also explored for managerial insights.

The thesis is structured as follows. Chapter 2 reviews the main literature, addressing topics related to this research, specifically including hazmat transportation, bilevel modeling, and network design. Then, Chapter 3 outlines the mathematical formulations and various features, focusing on the bilevel structure of the problem to represent the conflicting interests of the parties involved. Building upon that, Chapter 4 describes solution algorithms, an exact method, for medium-scale problems, and a heuristic algorithm, suitable for very large problem instances. Their performances are tested and compared. In Chapter 5, one of the solution methods is then applied to the transpiration network of the city of Nanchang, China, illustrating the behavior of the proposed model within the context of a real life network and exploring the solutions under different circumstances as a case study. Finally, Chapter 6 concludes the research completed, outlining the main findings and proposing some possible areas to explore for future research.

Chapter 2

Literature Review

This chapter reviews the main research completed related to the topics this research emphasizes, covering the following topics: (1) Hazmat Risk, focusing on the measurement of risk, (2) Emergency Response, exploring the impact of responses to hazmat accidents to reduce consequences on the surrounding area, (3) Bilevel models, and their applicability to problem formulation, and (4) Hazmat Transportation Network Design, outlining the characteristics of designing networks specifically for hazamt transportation.

2.1 Hazmat Risk

The US Federal Motor Carrier Safety Administration, agency within the US Department of Transportation, defines hazardous materials as materials "posing an unreasonable threat to the public and environment" (US FMCSA, 2019) and require special care when being transported to reduce the likelihood of accidents. The accident probability of hazmat is very low, with an estimated accident probability between 10^{-8} and 10^{-6} per mile (Abkowitz and Cheng, 1988). Hazmat resulted in a total of 155,891 accidents, 1,335 injuries and 93 deaths on US highways from 2011 to 2020 (US PHMSA (2021)). However, the damages can be quite catastrophic, with approximately $632M in damages during the preceding time period according to the same report.

Based on the review done by Erkut et al. (2007), there exist a number of different ways to quantify the risk of hazardous materials. The main ones are outlined below. Here p_i represents the probability of an accident on link i within the set of links P, with c_i being its consequence.

Incident Probability. This approach, first explored in Saccomanno and Chan (1985), quantifies risk according to the relative frequency of an accident occurring on a road segment. Here, the total incident likelihood on the whole network is simply the sum over all the road links.

$$IP = \sum_{i=1 \in P}^{n} p_i \tag{2.1}$$

The main issue is that this measure fails to take into account the impact of an accident, as incidents are all given the same weighting. Therefore, IP works best for networks having road segments with similar profiles in terms of potential consequences.

Population Exposure. Another way of assessing risk is by quantifying the impact an accident has on a road link, measuring the overall risk by adding all the possible consequences (Batta and Chiu, 1988). Differently than the Incident Probability approach, PE fails to take into account the probability of an event happening. The same weight is given to a rare accident having considerable consequences, as to a more frequent event with a small impact. Nevertheless, this approach can help minimize the worst possible impact an accident could have, regardless of the chances of that happening.

$$PE = \sum_{i=1 \in P}^{n} c_i \tag{2.2}$$

There are different ways of assessing the impact an accident may have on the surrounding environment; a common is to employ a fixed bandwidth around a network edge (λ-neighborhood) (ReVelle et al., 1991). Other measures include an impact area modelled around the Gaussian plume model, taking into account external factors such as wind (Patel and Horowitz, 1994), or a circle with a hazmat-dependent radius around the accident location (Erkut and Verter, 1998).

The impacted population PE is generally used when talking about consequences, although other factors such as economic and environmental impact can be incorporated as well (Erkut et al., 2007).

Traditional Risk. Batta and Chiu (1988) further explored the idea of measuring risk by taking into account both the probability of an event happening and its consequences, giving the following equation to analyse risk:

$$TR = \sum_{i=1}^{n} p_i c_i \tag{2.3}$$

This combines both the Incident Probability and Population Exposure methods, providing a commonly used and generalized approach to quantify the risk on a network.

It is interesting to note that this is a simplification of the actual risk incurred on route, as TR assumes that all segments are independent and their probabilities do not depend on whether a carrier has made it this far. An exact model would take into account the possibility that an accident has not occurred on any of the previous segments. Because those values are very small, it is a realistic and practical approximation.

Perceived Risk. Abkowitz et al. (1992) proposed a way of adjusting the assessment of risk by accounting for the population's perception of risk, as opposed to a strictly technical calculation. The following equation is used:

$$PR = \sum_{i=1}^{n} p_i (c_i)^k, k > 0 \tag{2.4}$$

A "risk preference" factor k expresses the preference towards risk, with $k = 1$ being a risk-neutral position and $k > 1$ a risk-averse position, where the perception of risk of accidents having considerable impact is amplified.

Conditional Risk. Similar to PR, risk can be expressed as a function of the probability that an accident has happened on that route Sivakumar et al. (1993).

$$CR = \frac{\sum_{i=1}^{n} p_i c_i}{\sum_{i=1}^{n} p_i} \tag{2.5}$$

Through the equation above, CR attempts to overcome a limitation of the Traditional Risk that does not account for multiple hazardous materials being transported at once, in which case an accident would impact differently the various carriers using the route.

Maximum Population Exposure. More conservatively, risk can be measured as the maximum consequences an accident could have, with the goal of minimizing that value (min max expression), as shown by Erkut and Ingolfsson (2000). This is especially relevant when dealing with materials that could have catastrophic consequences on the population surrounding the environment. The following can be used:

$$MPE = \max c_i \tag{2.6}$$

Mean-Variance. Moreover, Sivakumar and Batta (1994) introduced the idea of minimizing the variance together with the Traditional Risk, making the risk more uniform throughout the network and ensuring the variance to be within a predefined threshold. On the hand, lower variance could come at the cost of increased overall TR. The following formula describes MV:

$$MV = \sum_{i=1}^{n} (p_i c_i + k p_i c_i^2), k > 0 \tag{2.7}$$

Expected Disutility. Another approach suggested by Erkut and Ingolfsson (2000) uses a risk-averse disutility function involving the number of casualties an accident would cause.

$$ED = \sum_{i=1}^{n} p_i \exp(k c_i - 1), k > 0 \tag{2.8}$$

This values exponentially increases by each additional person involved, allowing a reduction in the risk of accidents having a catastrophic impact with a high number of people.

Value at Risk (VaR). Originally used in in financial markets, Value at Risk (VaR) can be defined as the potential loss of capital for a given confidence interval and period of time (Jorion et al., 2007). Within the context of hazmat transportation, this can be

translated into the maximum potential risk associated with an accident within a certain confidence interval over a set of hazmat shipments, Kang et al. (2014*a*) and Kang et al. (2014*b*) explored this topic extensively. The following equation can be used to model the Value at Risk:

$$VaR^l_{\alpha i} = \min\{\beta : Pr\{R^l_i > \beta\} \leq 1 - \alpha\} \tag{2.9}$$

Where $\alpha \in (0, 1)$ is the confidence interval, β the VaR for shipment i on path l. Then, minimizing VaR^l_i yields the paths that ensure the Value at Risk is below the set threshold for the given confidence interval α. However, this average fails to account for events that have a very low probability (events in the "tail" of the distribution), but that could prove to be catastrophic in terms of consequences.

Conditional Value at Risk (CVaR). This method allows us to evaluate the expected accident consequence, given that it is greater than or equal to VaR, making it an extremely risk-averse technique. Moreover, this approach helps to lessen the worry that VaR cannot properly deal with very low probability events. Furthermore, CVaR problems are easier to solve than VaR problems because of convexity, as explained by Kwon (2011). CVaR is calculated as follows:

$$CVaR^l_{\alpha i} = \frac{1}{\alpha} \int_0^{\alpha} VaR^l_{\beta i} d\beta \tag{2.10}$$

where VaR is calculated following the expression listed above. Hosseini and Verma (2018) applied the same method for the transportation of hazmat materials by rail, showing CVar to be an appropriate way of measuring risk because of the more catastrophic nature of rail transportation, potentially involving multiple railcars in an accident.

Environmental Risk. Additionally, because of the nature of hazardous materials and the impact those could have on the environment surrounding an accident, risk can be evaluated with respect to the consequences on the environment. There has not been extensive research conducted on this topic, as most research emphasizes the potential harm to the population. Zhao and Verter (2015) used a 3-dimensional approach to assess the impact of the airborne hazmat of used oils, providing two measurements (for accidents at

a node and on an edge respectively). Together with a dispersion coefficient to account for atmospheric factors, Zhao and Verter (2015) argued ER better captures the spread of materials in all directions. Similarly, Zhao and Ke (2017) proposed a "volume-based explosion risk assessment" for waste that accounts for the potential explosive power of the material using volume. Zhao and Verter (2015) proposes the following risk formulation of a node and edge respectively:

$$B^{node} = \frac{1}{2} \times \frac{4}{3}\pi(R^{node})^3 \tag{2.11}$$

$$B^{edge} = \frac{1}{2} \times \pi R^{edge} D^{edge} \tag{2.12}$$

where B^{node} and B^{edge} represent the box shaped risk function of a node and edge, R^{node} and R^{edge} are the impact radius and D^{edge} is the distance of the edge.

Time-Based Risk.

Toll policies, a common approach for designing hazmat suitable networks, offer a method where all the road links can potentially be used, but a toll is applied to shape the desired shipment routing to minimize the risk according to the assessment method employed. For instance, if it is not desirable for carriers to be using a specific road link, then a high toll would be applied on that section to discourage carriers from using (as that would increase their transportation costs). Time-based risk calculations can be used to help authorities determine the correct toll policies to apply on the network. Wang et al. (2012) first introduced this method by examining the traffic flow through a single-level dual toll policy (one for hazmat and regular traffic) model to reduce risk through better management of traffic congestion, decreasing the risk of accidents occurring and their consequences. The idea is that an increased time spent on a road link will increase the associated risk. Some methods proposed include modelling risk as a "duration-population-frequency" expression that linearly depends on the hazmat carrier's time spent on a link, the traffic flow, as well as the population exposure (Wang et al., 2012), modelling risk as non-linear function (expression used by the US Bureau of Public Roads) as it better represents traffic congestion on a road link.

Additionally, response time can greatly influence the risk associated with an accident; this is further explored in the section 3.1.2 below. Taslimi et al. (2017) proposed incorporating response time into the decision model with the following measurement of risk:

$$\eta_i^k = \rho^k l_i \xi_i^k(f_i^m) \tag{2.13}$$

η_i^k represents the risk associated with a shipment of hazmat type k on link i, ρ the per-mile accident probability, which together with the l_i (length of segment i,) give the total accident probability on the link. ξ_i^k, a Response Time Factor (explained in more detail in the next section), is a time-dependent accident consequence for hazmat of type k function depending on f_i^m, the average response time from response team at m to link i. ξ_i^k is defined as being linearly dependent on the time from the response team's location to the accident location on link i, with the following:

$$\xi_i^k = q_i^k \frac{f_i^m}{F_i^k} \tag{2.14}$$

where $F_i^k > 0$ is a scaling constant depending on the hazmat type. This implies that with a slow response ($\frac{f_i^m}{F_i^k} > 1$) the accident consequences linearly increase with time. To the best of our knowledge, this is the first time such a formulation is included as part of the risk assessment. A similar formulation is used in the model proposed.

Following a similar idea, Zhao and Ke (2019), used full and partial coverage of an accident site, depending on its location with respect to the location of a response team, with the following risk expression:

$$R_i^k = \alpha \times PRO_i \times POP_i^k, \alpha \geq 0 \tag{2.15}$$

where PRO_i is the accident probability on link i, POP_i the exposed population, and $\alpha = 1$ for fully covered links and $\alpha > 1$ for partially covered links.

2.2 Hazmat Emergency Response

The degree to which an accident impacts the surrounding area, whether in terms of population or environment, can be greatly reduced with a timely response from a specialized

Hazmat Response Team (HRT), whose role is to control the spill of hazardous material. Transportation Research Board and National Academies of Sciences, Engineering, and Medicine (2011) provided a detailed overview regarding how to be appropriately prepared and respond to an accident. It identifies a "response time factor" (RTF), which indicates how well the response capabilities can deal with the accident and considers the assessment, management, rescuing and control of the accident. Moreover, the Response Time Factor covers the time it takes to report the accident, for first responders to arrive and finally for the HRT to arrive and start managing the accident. It also is important to note that different types of materials require different response capabilities from the response teams.

Within the same report, the accident consequences are defined as:

$$C = C_u \times ERC \times RTF \tag{2.16}$$

where C is the consequence, C_u is the unmitigated potential consequences, and ERC the Emergency Response Capability. Here we can note that the accident consequence, assuming an appropriate response capacity, is dependent on the response time. In other terms, the faster the response from the emergency team, the lower the consequences from the accident.

Response efficiency to accidents is a very effective strategy to mitigate the consequences; strategically placing emergency response teams to reduce response time greatly contributes to increasing their efficiency. Covering models have been proposed over the years as solution approach. For example, Church and ReVelle (1974) first maximized the coverage of service (maximal covering model), while setting a maximum distance from the desired facility location, ReVelle et al. (1976) focused on the application of the maximal arc-covering model formulated as a set covering problem, and Church and Meadows (1979) extended it to the form of a maximal covering location problem for locating facilities anywhere on the network.

With specific hazmat applications, Saccomanno and Allen (1987) presented a minimal set covering problem that imposes a minimum coverage level to locate emergency response teams, whose response capabilities are set according to the risk imposed by hazmat on the network. Later, List (1993) proposed a model minimizing the response time while imposing

certain maximum acceptable risk levels. List and Turnquist (1998) applied a multiobjective model (routing-siting model) to route hazmat and locate emergency response teams, specifying the shipment paths and locate a predefined number of facilities to minimize response time based on the traffic flow. Furthermore, Hamouda et al. (2004) developed a model to minimize the overall risk on a network, while maintaining service time below a certain time limit.

More recently, Berman et al. (2007) evaluated hazmat emergency response as a maximal-arc covering location, with the risk being measured in terms of population exposure on an edge. Given a maximum number of response teams, the model locates them on a subset of network nodes to maximize the total arc length covered, weighted by population exposure. Arcs are partially covered by HRT located at nearby nodes if they are within a certain time threshold. Zografos and Androutsopoulos (2008) assumed the demand on a road segment to be aggregated at its midpoint, making a node the midpoint between two road segments, and defining an arc as the road segment between two consecutive midpoints. A system is proposed to efficiently locate the hazmat response teams, as well as defining hazmat routes to minimize cost and risk in a first phase. The model then determines the optimal deployment of the response teams to an accident and provides evacuation routes from that location.

Then, Jiahong and Bin (2010) offered a multi-objective mixed integer linear programming model to locate emergency response teams to respond to hazmat accidents by adding the minimization of cost and transportation time as new objectives to a maximal arc-covering model. Moreover, Taslimi et al. (2017) examined the coverage of predefined zones on the network that cover one or multiple arcs or nodes, together with the surrounding area. A "consequence function" is developed based on the λ-neighborhood of an edge where the consequences of an accident linearly increases with response time, claiming damages could extend beyond the established λ-neighborhood if the response time is slower than the predefined value. Additionally, Zhao and Ke (2019) proposed a two way division (full and partial) of coverage to express the coverage capabilities a response team could have with respect to an accident at a specified location. Full coverage indicates a potential accident location is within a predetermined amount of time of a response team, and partial coverage is used for values greater than that; the model is employed to determine a response time

factor to assess risk, as mentioned in the previous section.

Generally, location models account for the average response time between two locations when optimizing for the placement of some sort of facility (distribution center, service center..). However, this fails to take into account that travel time often cannot be assumed to constant, especially when analyzing traffic flow on transportation networks. For example, Xu et al. (2013) developed a bilevel model with maximal-arc covering by considering risk as a Fu-Fu variable (a fuzzy variable having fuzzy parameters for vaguely defined properties) through a risk-reduction objective function.

2.3 Hazmat Transportation Network Design (HTND)

Hazmat Transportation Network Design (HTND), sometimes also called the Hazardous-Network Design Problem, describes the process of designing a network that is suitable for the transportation of hazardous materials. Such a network is generally designed to meet specific risk criteria to reduce the impact on the surrounding environment (population, for example). Two main approaches can be considered: closing links on an existing network to allow only specific segments to be available for hazmat transportation, and, besides that, expanding the network through the addition of new road links.

What characterizes this problem is the presence of two independent parties (government and carriers) with different goals, and the fact that their respective decisions influence each other. Moreover, the dynamic between those groups is also important. The government is in a dominant position when making the decision of how to structure the network (but cannot unreasonably dictate which road segments carriers can use within the hazmat network). The carriers follow the decision made by the authorities, with the freedom to choose whatever path results in the lowest cost to move from origin to destination using the available road segments. The latter must be considered by the government authority when designing the network.

First used by Kara and Verter (2004) to solve hazmat transportation problems, bilevel models are suitable to represent the transportation of hazardous materials on a network, outlining different objectives of the parties involved. In this case, government agencies

(upper-level) aim to minimize the impact of the transportation of such goods on the population and environment, and have the authority to do so. On the other hand carriers are looking to minimize their costs and ultimately determine the risk incurred by the network, based on the routing chosen.

A number of models and solution methods have been proposed over the years to represent the hazmat transportation network design problem. In the same paper, Kara and Verter (2004) proposed a model where the government designs a unique network for each hazmat category (classified according to risk); the carriers within each group are free to choose the route they wish within the available links. A solution is found by converting to a single-level problem through the Karush–Kuhn–Tucker (KKT) conditions.

Similarly, Erkut and Alp (2007) proposed a more computationally efficient model that creates a single possible route available for each origin-destination shipment pair (minimally connected tree). This effectively limits the route options for the carriers to a single one and simplifies the risk assessment. More links are then added through a heuristic method.

Building upon that, Erkut and Gzara (2008) expanded the problem to the undirected case and analyzed it for the worst risk, solving through transformation to a single-level model using duality and a heuristic method. Gzara (2013) obtained a solution through an exact cutting plane algorithm, consisting of identifying infeasible solutions to the bilevel problem in order to construct feasible ones. These are then added to the upper-level problem (decision of road segments to open/close to minimize risk) to iteratively solve the upper and lower-level. More recently, Taslimi et al. (2017) proposed a pessimistic model that integrates the location of emergency response teams within the hazmat transportation risk equity framework through a min-max objective.

Criticized as being too rigid, closing specific road links might be a waste of resources as a number of potential arcs are left unused. To overcome this, toll setting policies can be applied to a road network instead. For a more thorough review of that topic, see Ke et al. (2020).

2.4 Pessimistic Bilevel Models

Here we review the literature concerning bilevel models, focusing on the pessimistic formulation of the problem.

2.4.1 Bilevel Models

Bilevel models represent a class of decision-making problems that involve a hierarchical relationship between two decision makers (upper and lower level) where the decisions made by the two parties depend on each other, with the upper body having the freedom to take any action, but must consider the reaction of the lower-level, and whose decision constrains the possible solution of the lower-level (Sinha et al., 2017).

First introduced in 1934 by Heinrich Freiherr von Stackelberg (original: Von Stackelberg (1934), translated: Stackelberg et al. (1952)), this problem structure is also commonly referred to as Stackelberg game. The analysis focused on an economics perspective, examining the relationship and outcome of a leader firm having an advantage by moving first within the market and the follower firms moving sequentially (Von Stackelberg, 2010). Within the context of the problem analyzed, the upper-level body is a government agency, deciding which road segments in a network are available for hazmat transportation and the location of HRT on the network nodes; the lower-level body is the set of carriers aiming to minimize their transportation costs. Specifically, a pessimistic approach is taken, where the solution must account for the worst risk the hazmat carriers impose on the network (explained in more detail below).

Mathematically, a bilevel model can be represented as a problem whose solution depends on another set of problems, which in turn depends on the solution provided by the first problem; in other words, the upper-level (U) includes a constraint depending on the lower-level (L) problem. On the other hand, the decision made by the upper-level is included in the lower-level in the form of a constant (Bracken and McGill, 1973). It can be expressed with the following formulation (Dempe, 2020).

Let (L) be the lower-level, or follower, problem, defined as:

$$\text{(L)} \qquad \min_{y}\{f(x,y) : g(x,y) \leq 0, (x,y), y \in Y\} \tag{2.17}$$

with $Y \subseteq \mathbb{R}^n$ and defining $\phi(x)$ to be the optimal value of the above problem (depending on the value x set by the upper-level), the optimal value function of the lower-level can be defined accordingly

$$\Psi(x) := \{y \in Y : g(x,y) \leq 0, f(x,y) \leq \phi(x)\} \tag{2.18}$$

Abbreviating the graph of solution set mapping Ψ as gph Ψ (gph $\Psi := \{(x,y) : y \in \Psi(x)\}$), the upper-level (U), or leader, problem can be formulated

$$\min_{x}\{F(x,y) : G(x) \leq 0, (x,y) \in \text{gph } \Psi, x \in X\} \tag{2.19}$$

with $X \subseteq \mathbb{R}^m$. Here (U) has an objective function F and a decision variable x, with a constraint G depending on both x only. The lower-level (L), has an objective function f and a decision variable y, with a constraint g depending on x and y. For every value of x, the lower-level problem has a definite optimal objective value. Note that this represents the optimistic, or weak, formulation of the problem.

Bilevel problems are generally hard to solve, in fact these are NP-hard problems (Bard, 1991), and it is possible that even under good circumstances an optimal solution to a bilevel problem may not exist. Moreover, the complexity increases when dealing with bilevel integer programming problems (Jeroslow, 1985).

A number of solution methods have been proposed over time. Commonly used in the context of hazmat transportation network design and applied to the model presented, single-level reduction converts the bilevel problem to one for a single-level by transforming the lower-level problem into a set of constraints, either through KKT conditions (Bard and Falk, 1982) or duality (Marcotte et al., 2009), to be integrated into the upper-level problem.

Other approaches include gradient descent, where the upper-level objective function is improved while keeping the lower-level problem feasible (Kolstad and Lasdon, 1990), or via a penalty function, where a penalty cost is added to the unconstrained problem (Aiyoshi and Shimizu, 1981), and trust region for nonlinear models (Marcotte et al., 2001).

A solution to the bilevel problem, in the context of hazmat transportation, is deemed feasible if it is stable, that is. if the network does not allow for multiple minimum-distance paths having different risk values for any shipment (Amaldi et al., 2011).

2.4.2 Pessimistic Formulation

One of the issues of bilevel programs is that often the uniqueness of a solution in the lower-level cannot be guaranteed, leading to multiple optimal solutions due to an ambiguous formulation of the problem. Two approaches can then be taken to define the problem: an optimistic or a pessimistic one. In the first case, the optimistic formulation assumes that the lower-level body will always choose the optimal solution resulting in the best outcome for the upper-level problem. This often fails to account that the behavior of lower-level might deviate from the anticipated actions. This is problematic, as it does not provide a solution that is capable of dealing with potential changes and will only work as expected under the best circumstances. This is often not acceptable when examining risk, as the decision makers are often risk-averse and solution is expected to take into consideration the worst possible outcome.

On the other hand, a pessimistic bilevel model is a model that assumes that the lower-level will always choose, given multiple options with the same value, the outcome that would impose the worst outcome on the upper-level (Cao and Leung, 2002). The upper-level body must then take into account this factor and solve for a solution that would be acceptable under the worst-case scenario. Following the notation from the previous section, the pessimistic formulation can be defined with:

$$\min\{\phi_p(x) : G(x) \leq 0, x \in X\} \tag{2.20}$$

where

$$\phi_p(x) = \max_y \{F(x, y) : y \in \Psi(x)\} \tag{2.21}$$

Conversely to seeking a minimum lower-level value, here the lower-level is maximized to model the worst possible response from the follower. This is equivalent to a min max objective.

Pessimistic problem are generally harder to solve as, for example, the feasible region depends on optimality conditions of the lower-level, which might not be convex (Lozano and Smith, 2017), or a reduction to a single-level problem may not be possible (Sinha et al., 2017).

Recent work proposed an algorithm to solve an ϵ-approximation instance of the problem, converging to a solution with $\epsilon \to 0$, that allows for integer variables in the model and non-convexity (Wiesemann et al., 2013), Zheng, Fang and Wan (2016) applied a K-th best algorithm solution method, Dempe et al. (2014) derived necessary optimality conditions for general pessimistic bilevel problems, and Lozano and Smith (2017) outlined an exact finite algorithm, also applicable to optimistic models.

Following an idea similar to ϵ-approximation, *satisficing* behavior can be examined. First introduced by Simon (1956), it describes pursuing a solution to a problem that is considered "good enough", whose value is deemed satisfactory by the user when within a certain threshold, as opposed to finding an optimal solution. Moreover, users may be indifferent to alternative solutions of the problem when those are satisficing. This supports a pessimistic formulation, as it allows lower-level solutions (carrier routing) that are within the time/distance threshold. Minimization of the maximum risk exposure is then attempted, assuming users choose the riskiest path among the possible alternatives. Guo and Liu (2011) incorporated a bounded rationality threshold parameter (ϵ) into the model to represent possible alternative routes. Takalloo and Kwon (2020) used a similar parameter to assess the price of satsficing (the deviation from a perfectly rational approach), arguing that a satisficing solution is more realistic, but worse off than than an optimal one.

Pessimistic bilevel model have been applied to a number of different areas. Some of these include second best toll pricing to minimize some certain objective under a worst

case scenario to determine tolls on road links (Ban et al., 2009), interdiction games (drug smuggling, defense infrastructure, attacker-defender problems) often have a leader that desires to minimize the maximum consequences the follower could cause (Wood, 2010), (Liu et al., 2018), production planning to account for the lack of complete information across an organization to determine production and minimize costs (Zheng, Zhang, Han and Lu, 2016), or venture investments, where the leader needs to account for potentially conflicting interests within the different departments to maximize profit (Zheng, Zhu and Yuan, 2016).

When considering a pessimistic bilevel problem to evaluate the risk of hazmat transportation on a network, when multiple paths with the same cost (distance, time, toll etc.) are optimal for a carrier in the lower-level, then the path with the highest risk would be chosen, and attempts would be made to minimize the risk the resulting problem that minimizes the maximum possible risk for all shipments. However, if an optimistic approach were taken, the upper-level entity could encounter a much different risk exposure on the network, as the carriers could choose routes that have substantially higher risk than anticipated.

With specific hazmat applications, Amaldi et al. (2011) imposed a penalty on the lower-level objective function to seek a pessimistic solution, thus guaranteeing hazmat carriers would choose the path having maximum risk when two shortest paths are possible. That ensured an exact pessimistic solution to the problem, solving it by transforming to a single-level problem. Similarly, Fontaine and Minner (2018) used the same penalty method, applying decomposition for a more rapid solution of the problem. Both of those methods consider pessimism, however, to the best of our knowledge, no model applies a pessimistic bilevel model formulation to hazmat transportation. We propose a model with such structure.

2.5 Literature Gaps and Positioning of the Present Work

There has been an increasing amount of research done over the past few years regarding the risks related to the transportation of hazardous materials. However, there still lacks of a comprehensive investigation of how the hazmat carrier's worst behavior can impact the authority's network design decision, how the uncertain response time can be taken into account when determining the best location of emergency response teams, and in the end, how the system risk can be well controlled integratively. To fill these gaps in the literature, we herein propose a pessimistic network design problem with HRT locations considering uncertain emergency response time.

One research in the literature, Taslimi et al. (2017), dealt with a similar hazmat network design problem with HRT locations. That work differs from ours in the risk assessment and problem formulation, the candidate locations of emergency response teams, and how the model accounts for uncertainty. A detailed comparison between the two studies in summarized in Table 2.1. As indicated, we both aim to assess and minimize hazmat risk on a network through hazmat transportation network design and the location of emergency response teams to cover potential accidents in an optimal way. But Taslimi et al. (2017) also overlooked the carriers' behavior and the uncertainty prevailing in the emergency response process.

To be specific, our contributions are described as follows.

1. Because cooperation between regulatory bodies and shipment carriers cannot be guaranteed, a pessimistic bilevel model is adopted. Most models pertaining to the risk assessment of hazmat transportation, perhaps as a simplification mechanism, use an optimistic formulation and overlook the possible deviation of carrier's behavior from the expected. We believe to be the first to develop such an approach for hazmat transportation.

2. Similar to Taslimi et al. (2017) and due to a perceived lack of research accounting for emergency response effectiveness in the assessment of risk, we integrate a measure of

Table 2.1: A Comparison Between Taslimi et al. (2017) and the Present Research

	Taslimi et al. (2017)	Present Research
Model Structure	Bilevel model	Pessimistic Bilevel model
Risk Assessment	Risk equity, minimizing the maximum risk of any given zone through a min max expression	Pessimistic approach to minimize the maximum network risk, also accomplished through a min max expression applied to the overall risk
Network Design	Define availability of road links for hazmat transportation. Additionally, new links can be added to the network	Hazmat network defined solely based on the availability for hazmat transportation of existing links
Response Team Location	Location of HRT at specified candidate locations for coverage of a single zone of the network (road links, nodes and surrounding areas). RTF is integrated within the objective	Location of HRT possible on any network node, with a response team having the ability to potentially cover any road link. More locations are available (bigger problem) and more coverage options for the arcs, as the coverage is not limited to the response team within the area. RTF is integrated within the objective
Uncertainty	Uncertainty in model parameters analyzed by examining possible boundaries and performing simulations to obtain a more robust solution	Uncertainty considered as a probability distribution of response time to accidents. Constraints in the model directly account for this to ensure pre-specified service level and constraint the network design and HRT location
Solution Method	A single-level representation and a greedy heuristic approach for more complex problems	A single-level conversion and a 2-stage heuristic for more complex problems

emergency response time from HRT to accident location. This better represents the risk consequences, where a faster response diminishes the impact and contributes to minimizing risk.

3. Additionally, we account for uncertainty in the traffic flow by designing a network suitable for the transportation of hazmat that guarantees predefined service levels for accident coverage from emergency response teams.

4. Through the bilevel model, we outline an exact method together with a heuristic method to design the network. We place emergency response teams in a two-stage process that yields accurate solutions in a computationally efficient manner, targeted

for solving more complex problems.

5. Finally, we apply our models to a real transportation network in China to study it's effectiveness in designing an appropriate network and assessing the risk, and compare the computation and accuracy of the solution methods proposed.

The following chapter outlines our mathematical model in a pessimistic bilevel structure for a hazmat transportation network that accounts for the location of emergency response teams on any network node to contribute to the reduction of risk and ensures minimum response times to hazmat accidents on road links.

Chapter 3

Model

This chapter outlines the mathematical formulation of the model. The problem is introduced in Section 3.1, covering risk measurement, pessimistic formulation, the inclusion of uncertainty in the model and the location of emergency response. Section 3.2 describes the bilevel structure of the model, whereas the assumptions made are outlined in section 3.3. Finally, the notation and mathematical formulation of the model are introduced in Sections 3.4 and 3.5 respectively.

3.1 Problem Definition

Let $\mathcal{G}(\mathcal{N}, \mathcal{A})$ be a directed network with $\mathcal{N}$ being the set of nodes and $\mathcal{A}$ the set of arcs (all the links that could potentially be used by carriers for hazmat transportation). We define $\mathcal{C}$ as a set of shipments of size $|\mathcal{C}|$, with each shipment $c \in \mathcal{C}$ having origin node $o^c \in \mathcal{N}$ and destination $d^c \in \mathcal{N}$. It is assumed that there is at least one feasible path from o^c to d^c for each shipment c. Moreover, it is assumed that each shipment c transports one type of hazmat $k \in \mathcal{K}$ (with $\mathcal{K}$ being the set of all hazmats) Each k may have different properties in terms of probability of a spill after an incident and dispersion area of material transported.

3.1.1 Risk Measurement

The proposed model is based on the Traditional Risk approach (see Section 2.1). Here we define the risk as being a product of the population exposed and the probability that the population is exposed to hazmat after an accident. The following formula outlines the calculation:

$$Risk = q(k) \times \rho^k \tag{3.1}$$

Here $q(k)$ represents the population exposure to hazmat k, and ρ^k the probability of exposure to hazmat k after an accident. The population exposed is:

$$q(k) = A(k) \times PopDensity, \tag{3.2}$$

where $A(k)$ is the area around the accident point, considering a radius for the impact area. Because different hazmat types will behave differently and spread in a unique manner For example, gaseous materials will affect a wider area than a solid one, with a radius depending on k. Additionally, depending on the location of the accident, the area can be assessed differently. In the case of a node, the area can be expressed as circle with $A(k) = \pi r^2(k)$, and for edges a rectangle centered around the link can be used with $A(k) = r(k)l_{ij}$.

On the other hand, ρ^k, the probability that the population potentially affected ($q(k)$) is exposed to hazmat after an accident is defined as:

$$\rho^k = P(release(k)|accident) = \frac{P(release(k) \cap accident)}{P(accident)} \tag{3.3}$$

with $P(release(k))$ being the probability of hazmat being released and $P(accident)$ representing the probability that an accident occurs (also known as accident rate and estimated to be between 10^{-8} and 10^{-6} per mile (Abkowitz and Cheng, 1988)).

Because each shipment transports only one type of hazmat k, we can rewrite the risk as a function of the shipment instead of the hazmat type directly. To simplify the formulation, we define $R^c_{ij} = n^c l_{ij} q^k \rho^k$, n^c indicating the number of trucks, to describe the total risk imposed on a road link (i, j) for a shipment c of hazmat type k, assuming all shipments

to be independent of one another. The total risk on link (i, j) can then be calculated accordingly:

$$Risk_{ij} = \sum_{c \in \mathcal{C}} R_{ij}^{c} \tag{3.4}$$

Finally, the total risk the hazmat shipments impose on the network can be found with:

$$Network\ Risk = \sum_{(i,j) \in \mathcal{A}} \sum_{c \in \mathcal{C}} R_{ij}^{c} \tag{3.5}$$

3.1.2 Emergency Response

An appropriate response from a specialized team (Hazmat Response Team) can greatly reduce the impact of a hazmat accident on the surrounding environment (population, environment, etc..) and the pessimistic approach of the problem can be enhanced.

Response Time Uncertainty

Our research adopts an arc coverage model to determine the best location of the HRT on the network nodes. We define an arc (i, j) to be covered by an emergency response at node m if the travel time to the farthest point on the link (t_{ij}^{m}) is within a pre-specified travel time T_{max}, assuming the shortest path taken by the responders. Because risk increases with time (Taslimi et al., 2017), reducing the travel time between potential accident sites and HRT contributes to reducing the risk imposed on the network by hazmat carriers. Figure 3.1 depicts the coverage of an arc (i, j) from a hazmat location at m (node i) as the travel time $t_{ij}^{m} \leq T_{max}$ (maximum time allowed for coverage); link (j, j'), however, cannot be covered by the emergency response team at m as $t_{jj'}^{m} > T_{max}$. This can be written as

$$t_{ij}^{m} h_{ij}^{m} \leq T_{max} \qquad \forall (i, j) \in \mathcal{A}, \forall m \in \mathbf{N} \tag{3.6}$$

where $h_{ij}^{m} \in \{0, 1\}$ indicates whether an HRT at node m can cover link (i, j), allowing a response team to only provide coverage ($h_{ij}^{m} = 1$) if the travel time is lower than the

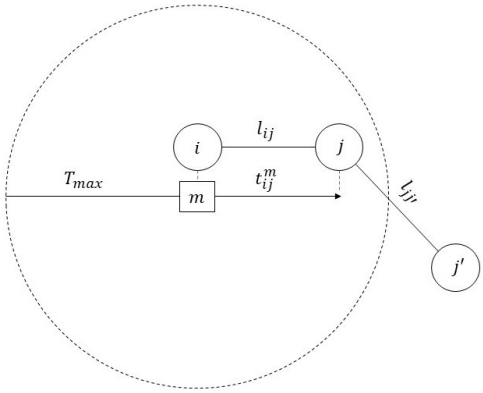

Figure 3.1: Arc Coverage

maximum response time. Additionally, an arc can be covered by only a single HRT, i.e.,

$$\sum_{m \in \mathcal{N}} h_{ij}^m \leq 1 \qquad \forall (i,j) \in \mathcal{A} \tag{3.7}$$

To provide reliable and consistent responses to accidents, traffic flow cannot be assumed to be constant by simply using the average value to describe the travelling time between two points on the network. Doing so would defeat the purpose of the pessimistic formulation, and result in the response time being greater than the specified value half of the time. To mitigate this and account for the uncertainty in response time, travelling time is examined as a probability distribution, defined as T_{ij}^m with mean t_{ij}^m and variance σ^2. To model the uncertainty in response time for the arc coverage model, we constrain the waiting time for a service to be below a set threshold in the following manner (Marianov and Serra, 1998):

$$P(T_{ij}^m h_{ij}^m \leq T_{max}) \geq \tau \qquad \forall (i,j) \in \mathcal{A}, \forall m \in \mathbf{N} \tag{3.8}$$

to ensure the response time to an accident to be below a set threshold T_{max} with probability at least τ. For example, setting $\tau = 0.95$, Eq. (3.8) guarantees that the response time from m to link (i,j) (assuming the response team is allocated to that arc with $h_{ij}^m = 1$) will be lower than the maximum time allowed at least 95% of the time.

To enhance the pessimistic formulation of the problem, two service levels are defined: the desired best, or optimistic, and the worst, or pessimistic, allowable response time, thus

accounting for the worst case scenario. For a link (i, j) to be covered by a response team at node m, i.e. $h_{ij}^m = 1$, both service levels must satisfied. Expression (3.8) can then be expanded to:

$$P(T_{ij}^m h_{ij}^m \leq T_{best}) \geq \gamma \qquad \forall (i,j) \in \mathcal{A}, \forall m \in \mathbf{N} \tag{3.9}$$

$$P(T_{ij}^m h_{ij}^m \leq T_{worst}) \geq \beta \qquad \forall (i,j) \in \mathcal{A}, \forall m \in \mathbf{N} \tag{3.10}$$

where T_{best} and T_{worst} are the pre-defined optimistic and pessimistic coverage times. Note that γ (optimistic) and β (pessimistic) indicate the probabilities that response times T_{ij}^m are below T_{best} and T_{worst} respectively. These guarantee that when a link (i, j) is covered by an HRT at node m, the response time will be less than T_{best} for $\gamma\%$ of the time as well as less than T_{worst} for $\beta\%$ of the instances. It follows that $\beta \geq \gamma$, and both values can be tuned according to the service levels required. Eqns. (3.9) and (3.10) can then be transformed into:

$$F^{-1}(\gamma) \leq T_{best} \qquad \forall (i,j) \in \mathcal{A}, \forall m \in \mathbf{N} \tag{3.11}$$

$$F^{-1}(\beta) \leq T_{worst} \qquad \forall (i,j) \in \mathcal{A}, \forall m \in \mathbf{N} \tag{3.12}$$

with F^{-1} as the inverse Cumulative Distribution Function (cdf).

The chance constraint is generally complex to solve as it is hard to evaluate the actual probability of an event, and the feasible set might not be convex. Many solution methods, include converting the problem to mixed-integer linear program with the use of big-M constraints, applying branch-and-bound algorithms, and modelling the problem as distributionally robust chance-constrained program that uses an ambiguity set, have been developed by various scholars (Küçükyavuz and Jiang, 2021).

As to the travel time between two points on a network, studies have done in terms of the goodness-of-fit of travel data for distributions, such as Weibull, Log-Normal, and Normal. Through examining large-scale data sets of various urban roads, Li et al. (2013) concluded that the Normal distribution can provide the most fitting estimate of the travel time between two points on a network under most traffic conditions. Therefore, we herein employ the Normal distribution to represent the uncertain response time. A chance constraint adopting a Normal distribution can be easily reformulated to be deterministic with known

parameters (namely the mean and standard deviation), and thus simplifies the solution method of the model.

Response Time Factor

Additionally, the response time influences the risk assessment, as faster responses reduce the consequences (Taslimi et al., 2017; Zhao and Ke, 2017). We herein take the idea from Zhao and Ke (2017) and introduce a Response Time Factor (RTF), $\alpha(t_{ij}^m)$ as a function in terms of the response time t_{ij}^m, into the objective function to reflect the time-relevant nature of the system risk. This factor helps in defining the shape of the risk curve on the network (which can be discrete, linear, or nonlinear), and can be estimated by the undesirability of the accident consequences, the capabilities of the response teams and environment. Note that the linear format of RTF proposed in Taslimi et al. (2017) (i.e., t_{ij}^m/T_{best}) can be unreasonable, as even an *immediate* response (i.e., $t_{ij}^m = 0$) would not diminish the impact of any incident, rather, only mitigate the spread rate of the harmful effect. Therefore, by setting the value of $\alpha(t_{ij}^m)$ to be no less than 1 (i.e., $\alpha(t_{ij}^m) = 1$ when $t_{ij}^m \leq T_{best}$; $\alpha(t_{ij}^m) > 1$ otherwise), we are able to more realistically address the time-relevant risk assessment in emergency response. A discussion about how to determine the value for $\alpha(t_{ij}^m)$ can be found in the case study in chapter 5.

We are taking a pessimistic approach, as it is assumed the government aims to minimize the worst risk on the network. Integrating the above RTF, the following min max expression is thus adopted.

$$\min \max \sum_{n \in \mathcal{N}} \sum_{(i,j) \in \mathcal{A}} \sum_{c \in \mathcal{C}} R_{ij}^c \alpha(t_{ij}^m) \tag{3.13}$$

This can then be linearized as:

$$\min \ \theta \tag{3.14}$$

$$\sum_{n \in \mathcal{N}} \sum_{(i,j) \in \mathcal{A}} \sum_{c \in \mathcal{C}} R_{ij}^c \alpha(t_{ij}^m) \leq \theta \tag{3.15}$$

Through this expression, the hazmat transportation network is designed in conjunction with the location of the emergency response teams to minimize the maximum network risk.

3.2 A Pessimistic Bilevel Model Structure

The problem analyzed involves two main parties: (1) government agencies responsible for regulating traffic of hazardous materials and (2) hazmat carriers in charge of transporting goods from origin to destination. A bilevel structure, depicted in Fig 3.2, is used to model the diverging objectives. In the upper-level, the government designs the hazmat transportation network by choosing which links of the regular transportation network are to be available for moving hazmat, and locates its emergency response teams at the nodes. The objective is to minimize the maximum risk of the network by taking into account the routing of the carriers, as well as the impact that HRT have in reducing the consequences of accidents.

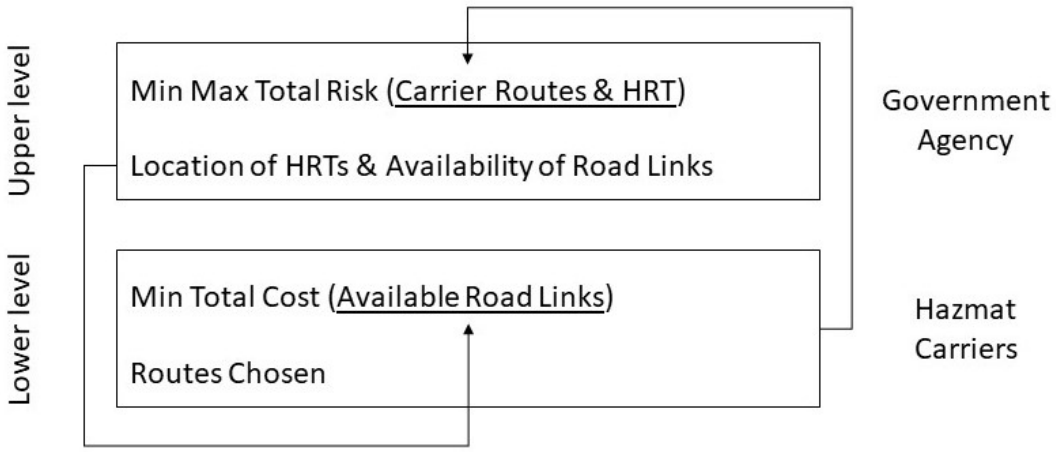

Figure 3.2: Bilevel Structure of Problem

The hazmat carriers are represented in the lower-level, where they are free to design the most convenient routes, based on the network provided by the upper-level, to minimize their costs of transportation in terms of travelling time. They do so regardless of the risk

imposed on the network and the surrounding areas.

Our model adopts a pessimistic stance to represent the government's desire to account for the worst possible risk on the network and design a suitable network and place emergency response teams accordingly. In practice, this means forcing the carriers to choose the route having the maximum risk, given that there exists multiple possible routes having the same distance and satisfying the carriers objective of minimizing distance travelled.

One of the peculiarities of bilevel models is the issue of stability, as the problem might not have an optimal solution. This is because the lower-level problem potentially has multiple identical optimal paths each with different risks, which may result in unexpected risks from the government's standpoint if specific routes cannot be enforced (Erkut and Gzara, 2008). A pessimistic formulation of the problem does not have this complication, as the government designs a network that accounts for the worst possible risk of the carriers, thus eliminating the possibility of multiple optimal paths having risks higher than expected.

The following compares pessimistic and optimistic approaches in more details, and their implications for network design and HRT location through a simple example.

Pessimistic and Optimistic Comparison

Consider a simple network with three nodes (Figure 3.3). The two values on each link respectively give the distance and risk of that link. To ship one unit of hazmat from A to C, two paths are available:

1. $A \to B \to C$ with a distance of 10 and risk of 20, and
2. $A \to C$ also with a distance of 10 yet a lower risk of 12.

Note that both paths have the same distance. Under an optimistic setting, the carrier chooses the one with lower risk, i.e., $A \to C$. However, the pessimistic model assumes the worst case, where the carrier does not cooperate by selecting $A \to B \to C$ with a higher risk. So to induce the carrier to $A \to C$, the authority can close link (A, B) (or link (B, C)) from the network design perspective.

When taking the HRT location into consideration, three candidate locations exist in this example. Assuming each location can reduce the risk of each connected link by half

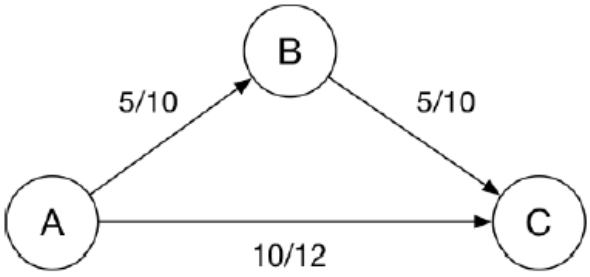

Figure 3.3: A simple example

but has no impact to other links, the resulting risks under different locations can be seen in Table 3.1.

Table 3.1: Cost/Risk with HRT

hrt	$A \to B \to C$	$A \to C$	opt selection	pes selection
None	10/20	10/12	$A \to C$	$A \to B \to C$
A	10/15	10/6	$A \to C$	$A \to B \to C$
B	10/10	10/12	$A \to B \to C$	$A \to C$
C	10/15	10/6	$A \to C$	$A \to B \to C$

Observing Table 3.1, the carrier under an optimistic setting chooses path $A \to C$ when an HRT is located at either node A or C, while selects $A \to B \to C$ with an HRT at B. Nevertheless, if the carrier behaves pessimistically, the network design approach needs to be implemented by the authority to force the carrier to the safer path. Similarly, closing link (A, B) (or link (B, C)) and locating an HRT at either A or C can do the job.

Two further points need to be pointed out. First, with the present risk values, path $A \to B \to C$ does work better when an HRT is built at B, but the resulting risk is still not low enough. Secondly, the above network decision also works when the risk for link (A, C) is lower than 10. In that case, path $A \to B \to C$ would be chosen under all possibilities. To avoid this selection, the same network action can be taken.

From the above discussion, we can see that the effectiveness of an optimistic model largely depends upon the best behavior of the carrier, which is extremely hard to be

predicted (if not impossible) by the authority. By applying the pessimistic model, the authority is able to manage the carrier's behavior by avoiding undesired selection and inducing the most preferred path through various mechanisms, such as the network design (closing certain links) in this work. At this point, it can also be noticed that while network design decisions lead the carrier to the desired path, the HRT location decision further mitigates the corresponding risk.

In the following section, we present the detailed mathematical formulation following the assumptions and notation.

3.3 Assumptions

Some assumptions are made in the model:

1. The impact of external traffic is not considered.
2. All nodes in the network can be considered as candidate locations for an HRT. Moreover, any link can allow the transportation of hazmat if permitted by the government.
3. We assume there is no cooperation, in the form of incentives for example, between the government agencies and the hazmat carriers.
4. Response teams do not have a capacity constraint. Due to the low accident probability, it is assumed all links that are available for hazmat transportation are usable by emergency response teams (no accident preventing the usage, for example).
5. The network is assumed to be uncapacitated, that is each road link could accommodate any number of shipments.
6. To simplify the model without loss of generality, it is assumed that a shipment c transports a single type of hazmat k. Multiple hazardous materials in the same shipment might interact in unpredictable ways and complicate the risk assessment. The model can, however, be applied for any single type of hazmat category.

3.4 Notation

Network and sets

$\mathcal{C}$:	set of shipments having origin o_c and destination d_c.
$\mathcal{K}$:	set of hazmat types.
$\mathcal{N}$:	set of nodes.
$\mathcal{A}$:	set of arcs, between pair of links i and j.
$\mathcal{G}(\mathcal{N}, \mathcal{A})$:	directed network constructed on $\mathcal{N}$ and $\mathcal{A}$.

Variables

y_{ij}:	availability of a link (i, j) for hazmat transportation, with $y_{ij} \in \{0, 1\}$.
v^m:	HRT located at node m, with $v^m \in \{0, 1\}$.
x_{ij}^c:	use of link (i, j) by shipment c, with $x_{ij}^c \in \{0, 1\}$.
h_{ij}^m	coverage of link (i, j) by HRT at node m, with $h_{ij}^m \in \{0, 1\}$.

Parameters

R_{ij}^c	from Section 3.1.1, $R_{ij}^c = n^c l_{ij} q^k \rho^k$, and describes the total risk of shipment c, transporting hazmat solely of type k, on link (i, j)
ρ^c:	probability of exposure to hazmat being transported by shipment c after an accident, based on hazmat of type k.
l_{ij}:	length of link (i, j), in km.
n^c:	number of shipments with origin $o(c)$ and destination $d(c)$.
q^c:	population exposure for accident of hazmat c.
$\alpha(t_{ij}^m)$:	coefficient of risk decrease when link (i, j) is covered by HRT.
γ:	optimistic coverage time probability.
β:	pessimistic coverage time probability.
θ:	maximum network hazmat risk.
t_{ij}^m:	average time from node m to link (i, j).

T_{ij}^m:	random distribution of travel time between node m and link (i,j) with average t_{ij}^m and variance σ^2.
T_{best}:	desired best case response time.
T_{worst}:	worst case response time allowed.
H:	maximum number of HRT that can be allocated on the network.

3.5 Mathematical Formulation

Following the bilevel model structure outlined in Section 3.2, the mathematical model is divided into upper-level and lower-level formulations. The above mentioned notation is used. We then write the formulation of the upper and lower-level problems, and the bilevel formulation can be found in Appendix A.

3.5.1 Upper-Level

The upper-level outlines the government agency's problem to design the hazmat transportation network and locate the emergency response teams. A min max objective is implemented, dictating the pessimistic formulation of the problem and reflecting the desire to design a network suitable for the worst case scenario. The hazmat carrier's shipment routing ultimately defines the risk imposed on the network, and is accounted for by a variable x_{ij}^c in the objective function.

We define the upper-level problem (U) as:

$$\min \quad \theta \tag{3.16}$$

$$\text{s.t.} \quad \sum_{m\in\mathcal{N}} \sum_{(i,j)\in\mathcal{A}} \sum_{c\in\mathcal{C}} R_{ij}^c \alpha(t_{ij}^m) h_{ij}^m x_{ij}^c \leq \theta \tag{3.17}$$

$$\sum_{m\in N} v^m \leq H \tag{3.18}$$

$$h_{ij}^m \leq v^m \qquad \forall (i,j)\in\mathcal{A}, \forall m \in \mathcal{N} \tag{3.19}$$

$$\sum_{m\in N} h_{ij}^m \geq x_{ij}^c \qquad \forall (i,j)\in\mathcal{A}, \forall c \in \mathcal{C} \tag{3.20}$$

$$\sum_{m \in N} h_{ij}^m \leq 1 \qquad \forall (i,j) \in \mathcal{A} \tag{3.21}$$

$$P(T_{ij}^m h_{ij}^m \leq T_{best}) \geq \gamma \qquad \forall (i,j) \in \mathcal{A}, \forall m \in \mathcal{N} \tag{3.22}$$

$$P(T_{ij}^m h_{ij}^m \leq T_{worst}) \geq \beta \qquad \forall (i,j) \in \mathcal{A}, \forall m \in \mathcal{N} \tag{3.23}$$

$$y_{ij} = y_{ji} \qquad \forall (i,j) \in \mathcal{A} \tag{3.24}$$

$$y_{ij}, h_{ij}^m \in \{0,1\} \qquad \forall (i,j) \in \mathcal{A}, \forall c \in \mathcal{C} \tag{3.25}$$

The min max objective is represented by Equations (3.16) and (3.17). The total risk on the network imposed by the routing choices made by the carriers (x_{ij}^c, with a value of 1 when link (i,j) is used by shipment c and 0 otherwise) is calculated, and accounts for the emergency response effectiveness when a link is covered (h_{ij}^m, α). The risk calculation follows the approach outlined in Sections 3.1.1 and 3.1.2. Note that the objective is not linear, as both x_{ij}^c and h_{ij}^m are binary variables.

The remainder of the model relates to the location of the emergency response teams at the nodes. Eqn. (3.18) limits the number of HRT that can be allocated to H, the maximum number permitted. Eqn. (3.19) ensures that a link (i,j) can only be covered by an HRT at node m if there actually is an emergency response team located at that node. Eqn. (3.20) indicates that if a link is used by a carrier ($x_{ij}^c = 1$), then it must be covered by an emergency response. Eqn. (3.21) limits a link to be covered by a single HRT. Additionally, Eqns. (3.22) and (3.23) account for the uncertainty in response time for a response team to attend to an accident, defining a best and worst service time following the approach outlined in Section 3.1.2. Naturally, because the HRTs are uncapacitated, a link will be covered by the closest emergency response team to minimize the response time and the associated risk. Finally, Eqn. (3.24) forces a link (i,j) to be available in both directions (from i to j and vice-versa). This constraint can be avoided by specifying the definition of variable y_{ij} with $i < j$ under a symmetric graph setting.

3.5.2 Lower-Level

The lower-level concerns the hazmat carriers and models their desire for minimum transportation costs. Those costs are formulated here in terms of total distance from origin o^c

to destination d^c. The network of possible links is the network designed by the government through the upper-level model.

We define the lower-level problem (L) as:

$$\min \quad \sum_{c\in\mathcal{C}} \sum_{(i,j)\in\mathcal{A}} \sum_{m\in\mathcal{N}} n^c l_{ij} x_{ij}^c \tag{3.26}$$

$$\text{s.t.} \quad \sum_{i\in\mathcal{N}:(i,j)\in\mathcal{A}} x_{ij}^c - \sum_{l\in\mathcal{N}:(i,l)\in\mathcal{A}} x_{jl}^c = \begin{cases} 1 & j = o^c \\ -1 & j = d^c \\ 0 & \text{otherwise} \end{cases} \quad \forall j \in \mathcal{N}, \forall c \in \mathcal{C} \tag{3.27}$$

$$x_{ij}^c \leq y_{ij} \quad \forall (i,j) \in \mathcal{A}, \forall c \in \mathcal{C} \tag{3.28}$$

$$x_{ij}^c \in \{0,1\} \quad \forall (i,j) \in \mathcal{A}, \forall c \in \mathcal{C} \tag{3.29}$$

The objective function (Eqn. (3.26)) simply aims to minimize the total distance of all the shipments using the network. Eqn. (3.27) establishes a feasible flow path for the carrier to take from point o^c to d^c, while and Eqn. (3.28) ensures that for a link (i,j) to be used by shipment c, it must have been made available of the transportation for hazmat by the government agency ($y_{ij} = 1$).

3.6 Higher Connectivity Model

The model formulation proposed ensures that if a link (i,j) is to be made available for the transportation of hazardous materials ($y_{ij} = 1$), then it must be covered by an emergency response team (Eqn. (3.20)) to ensure that all the arcs potentially used by carriers can have an adequate response. In order to be covered, a link must satisfy constraints Eqns. (3.22) and (3.23). This might cause some problem instances to be infeasible if the proper amount of resources is not provided (number of HRT for example), as the possible coverage given those resources is not sufficient for the shipments, or to have a solution where some sections of the network are disconnected from each other.

To account for these two potential issues, we can adapt the model to provide a more relaxed formulation. First, we remove Eqn. (3.20) to allow arcs to be available even if

those are not covered by an HRT. Then, we substitute the network risk assessment (Eqn. (3.17), with:

$$\sum_{m\in\mathcal{N}}\sum_{(i,j)\in\mathcal{A}}\sum_{c\in\mathcal{C}} R_{ij}^{c}\alpha(t_{ij}^{m})h_{ij}^{m}x_{ij}^{c} + \sum_{(i,j)\in\mathcal{A}}(1-\sum_{m\in\mathcal{N}}h_{ij}^{m})\sum_{c\in\mathcal{C}} R_{ij}^{c}\alpha_{max}x_{ij}^{c} \tag{3.30}$$

where the first term gives the risk for the covered links ($\sum_{m\in\mathcal{N}} h_{ij}^{m} = 1$) and the second is for the uncovered links ($\sum_{m\in\mathcal{N}} h_{ij}^{m} = 0$). Because the maximum consequences of an accident are limited due to a finite amount of hazmat being transported and because a response time cannot be guaranteed, we set the RTF of the uncovered links to be the maximum possible value (α_{max}) to represent the worst response time of the capped risk of an incident.

Adopting these constraints translates into a model that prioritizes model connectivity and ensures all shipments can have a feasible path form origin to destination, over ensuring all the links are covered by emergency response teams within the predefined times. We refer to this model variation as **MCN** (Model Connectivity), whereas we call the base model (without the aforementioned variations) as **MCV** (Model Coverage).

Chapter 4

Solution Methodologies

Bilevel models, the structure adopted for formulating this problem, are computationally difficult to solve as they are in fact NP-hard (Jeroslow, 1985). It is often challenging to find a solution to such problems, especially when taking a pessimistic stance.

Two different solution methods are proposed: (1) single-level reformulation by converting to a single-level linear problem, suitable for problems of reasonable size (Section 4.1), and (2) a heuristic algorithm that breaks the linearized problem into two parts, applicable for larger problem instances (Section 4.2). These are explained in detail throughout this chapter.

4.1 Single-Level Reformulation

The model we present is a non-linear pessimistic bilevel integer model, specifically only working with binary variables. A common technique to solve bilevel models is to convert it into a single-level problem, much easier to approach. First applied by Kara and Verter (2004) to hazmat transportation, it integrates new sets of constraints into the upper-level problem.

Transforming a bilevel problem into its corresponding single-level formulation allows one to obtain a global minimum. This method is applicable for obtaining exact solutions

of regular size networks, whereas larger problems cannot be solved to obtain a solution within an acceptable amount of time.

Two common ways of approaching this are by applying the KKT conditions, as used by Kara and Verter (2004), and employing duality, as presented by Amaldi et al. (2011) and utilized by Taslimi et al. (2017). We herein implement the duality method, which shows better computational performance over KKT in our preliminary numerical tests.

4.1.1 Duality

Let us apply the duality approach to the MCN model. We start by observing that the network we are considering is uncapacitated. The follower's problem (Section 3.5.2), an Integer Linear Program, can then be broken down into $|C|$ subproblems independent of each other, as we do not need to account for any resources to be shared among carriers. Each subproblem can be solved separately. Because of this, the constraints of the problem form a totally unimodular matrix that allows the integrality condition on $x_{ij}^c \in \{0, 1\}$ to be substituted with $0 \leq x_{ij}^c \leq 1, \quad \forall (i, j) \in \mathcal{A}, \forall c \in \mathcal{C}$ and maintain optimality (Taslimi et al., 2017). This results in the lower-level problem becoming a Linear Programming Problem (LP), whose dual problem can be found.

The strong duality theorem can be applied to obtain a formulation to substitute for the follower's problem, thus allowing us to integrate it within the upper-level problem and solve a single-level Mixed Integer Linear Program (MILP). The result is that the LP outlined above can be effectively replaced by ensuring primal feasibility (primal constraints) and dual feasibility (dual constraints), and the reverse weak duality inequality (essentially imposing that the dual and primal objective values be the same, i.e. the optimal value) (Amaldi et al., 2011). We then write these below.

Let π_i^c $(\forall i \in \mathcal{N}, \forall c \in \mathcal{C})$ and π_j^c $(\forall j \in \mathcal{N}, \forall c \in \mathcal{C})$ be the dual variables of constraints (3.27). These result in:

$$\pi_j^c - \pi_i^c \leq n^c l_{ij} + M(1 - y_{ij}) \qquad \forall (i,j) \in \mathcal{A}, \forall c \in \mathcal{C} \tag{4.1}$$

$$\pi_{d^c}^c - \pi_{o^c}^c \geq \sum_{(i,j)\in\mathcal{A}} n^c l_{ij} x_{ij}^c \qquad \forall c \in \mathcal{C} \tag{4.2}$$

where (4.1) is the duality constraint and (4.2) is the reverse weak duality inequality, which forces the primal and dual solutions to be the same.

4.1.2 Single-level Formulation

When integrating the constraints derived above, as well as equations (3.27) and (3.28), into the upper-level problem (U) (section 3.5.1), the single-level problem can be formulated as:

SLP:

$$\min \quad \theta \tag{4.3}$$

$$\text{s.t.} \quad \sum_{m\in\mathcal{N}} \sum_{(i,j)\in\mathcal{A}} \sum_{c\in\mathcal{C}} R_{ij}^c \alpha(t_{ij}^m) h_{ij}^m x_{ij}^c \leq \theta \tag{4.4}$$

$$\sum_{m\in\mathcal{N}} v_m \leq H \tag{4.5}$$

$$h_{ij}^m \leq v^m \qquad \forall (i,j) \in \mathcal{A}, \forall m \in \mathcal{N} \tag{4.6}$$

$$\sum_{(i,j)\in\mathcal{A}} h_{ij}^m \geq x_{ij}^c \qquad \forall (i,j) \in \mathcal{A}, \forall c \in \mathcal{C} \tag{4.7}$$

$$\sum_{(i,j)\in\mathcal{A}} h_{ij}^m \leq 1 \qquad \forall (i,j) \in \mathcal{A} \tag{4.8}$$

$$P(T_{ij}^m h_{ij}^m \leq T_{best}) \geq \gamma \qquad \forall (i,j) \in \mathcal{A}, \forall m \in \mathcal{N} \tag{4.9}$$

$$P(T_{ij}^m h_{ij}^m \leq T_{worst}) \geq \beta \qquad \forall (i,j) \in \mathcal{A}, \forall m \in \mathcal{N} \tag{4.10}$$

$$y_{ij} = y_{ji} \qquad \forall (i,j) \in \mathcal{A} \tag{4.11}$$

$$\sum_{i\in\mathcal{N}:(i,j)\in\mathcal{A}} x_{ij}^c - \sum_{i\in\mathcal{N}:(i,j)\in\mathcal{A}} x_{ji}^c = \begin{cases} 1 & j = o^c \\ -1 & j = d^c \\ 0 & \text{otherwise} \end{cases} \qquad \forall j \in \mathcal{N}, \forall c \in \mathcal{C} \tag{4.12}$$

$$x_{ij}^c \leq y_{ij} \qquad \forall (i,j) \in \mathcal{A}, \forall c \in \mathcal{C} \qquad (4.13)$$

$$\pi_j^c - \pi_i^c \leq n^c l_{ij} + M(1 - y_{ij}) \qquad \forall (i,j) \in \mathcal{A}, \forall c \in \mathcal{C} \qquad (4.14)$$

$$\pi_{d^c}^c - \pi_{o^c}^c \geq \sum_{(i,j)\in\mathcal{A}} n^c l_{ij} x_{ij}^c \qquad \forall c \in \mathcal{C} \qquad (4.15)$$

$$x_{ij}^c \in \{0,1\}, y_{ij} \in \{0,1\}, v^m \in \{0,1\}, h_{ij}^m \in \{0,1\} \qquad (4.16)$$

$$\pi_i^c, \pi_j^c \text{ free} \qquad (4.17)$$

All the variables are now determined simultaneously, causing the loss of total unimodularity of the constraints, for which we need to reimpose the binary conditions $x_{ij}^c \in \{0,1\}$.

We note that because of the interaction of h_{ij}^m and x_{ij}^c in constraint (4.4), the problem is not in a linear form. After having solved a number of instances of the problem, this results in slow computational time. To improve it, we can linearize the model by adding a new variable $w_{ij}^{cm} = h_{ij}^m x_{ij}^c$ and the following equations (Taslimi et al., 2017):

$$h_{ij}^m + x_{ij}^c - w_{ij}^{cm} \leq 1 \qquad \forall (i,j) \in \mathcal{A}, \forall c \in \mathcal{C}, \forall m \in \mathcal{N} \qquad (4.18)$$

$$h_{ij}^m + x_{ij}^c \geq 2w_{ij}^{cm} \qquad \forall (i,j) \in \mathcal{A}, \forall c \in \mathcal{C}, \forall m \in \mathcal{N} \qquad (4.19)$$

$$w_{ij}^{cm} \geq 0 \qquad (4.20)$$

and substitute constraint (4.4) with:

$$\sum_{m\in\mathcal{N}} \sum_{(i,j)\in\mathcal{A}} \sum_{c\in\mathcal{C}} R_{ij}^c \alpha(t_{ij}^m) w_{ij}^{cm} \leq \theta \qquad (4.21)$$

The MILP with the updated constraints can be found in Appendix B. It is interesting to note that Eqns. (4.18) and (4.19) can be substituted with $w_{ij}^{cm} > h_{ij}^m \forall (i,j) \in \mathcal{A}, \forall c \in \mathcal{C}, \forall m \in \mathcal{N}$ and $w_{ij}^{cm} > x_{ij} \forall (i,j) \in \mathcal{A}, \forall c \in \mathcal{C}, \forall m \in \mathcal{N}$ respectively. This alternative formulation has a comparable computation time.

Improved Linearization

SLP can be rewritten through a better linearization approach that uses a slightly lower number of variables to represent the problem. Here the variable h_{ij}^m becomes $h_{ij}^{mc} \in \{0,1\}$,

combining the utilization of the link by shipment c and the coverage through HRT at node m to indicate whether a link (i, j) is used by shipment c and covered by an emergency response team at node m. Variable w_{ij}^{cm}, together with constraints (4.18) and (4.19), are then removed from the model. We refer to this model as **SLPIL** (Single-Level Problem Improved Linearization). Table 4.1 compares the problem sizes, formed by the number of nodes ($|\mathcal{N}|$), number of arcs ($|\mathcal{A}|$) and number of shipments ($|\mathcal{C}|$), of SLP and SLPIL. We note there is a difference of $|\mathcal{N}| \times |\mathcal{A}|$ between the two models, with the latter having fewer variables, as variable w_{ij}^{cm} is removed while index c is added to h_{ij}^{m}. On the other hand, SLPIL has additional constraints, as the the new variable h_{ij}^{mc} now forces a number of constraints to be defined $\forall c \in \mathcal{C}$. These new added constraints are of larger quantity compared to the ones removed to linearize through w_{ij}^{cm}. These differences are outlined in Table 4.2. Both factors contribute to a lower computational time (see Table 4.5 for a more detailed numerical comparison).

Table 4.1: Problem Size Comparison of SLP & SLPIL

Variable	SLP (Index: Amount)	SLPIL (Index: Amount)
x	$c, (i, j) : \lvert\mathcal{C}\rvert \times \lvert\mathcal{A}\rvert$	$c, (i, j) : \lvert\mathcal{C}\rvert \times \lvert\mathcal{A}\rvert$
y	$(i, j) : \lvert\mathcal{A}\rvert$	$(i, j) : \lvert\mathcal{A}\rvert$
v	$m : \lvert\mathcal{N}\rvert$	$m : \lvert\mathcal{N}\rvert$
h	$m, (i, j) : \lvert\mathcal{N}\rvert \times \lvert\mathcal{A}\rvert$	$m, c, (i, j) : \lvert\mathcal{N}\rvert \times \lvert\mathcal{C}\rvert \times \lvert\mathcal{A}\rvert$
π	$c, j : \lvert\mathcal{C}\rvert \times \lvert\mathcal{N}\rvert$	$c, j : \lvert\mathcal{C}\rvert \times \lvert\mathcal{N}\rvert$
w	$m, c, (i, j) : \lvert\mathcal{N}\rvert \times \lvert\mathcal{C}\rvert \times \lvert\mathcal{A}\rvert$	-

Table 4.2: Problem Size Comparison of SLP & SLPIL - Example

Set Size			Number of Variables			Number of Constraints		
$\lvert\mathcal{N}\rvert$	$\lvert\mathcal{A}\rvert$	$\lvert\mathcal{C}\rvert$	SLP	SLPIL	Difference	SLP	SLPIL	Difference
25	100	10	28,875	26,375	2,500	59,962	78,262	-18,300
25	100	25	68,250	65,750	2,500	138,352	195,652	-57,300
25	100	50	133,875	131,375	2,500	269,002	391,302	-122,300
50	200	10	112,750	102,750	10,000	234,912	306,512	-71,600
50	200	25	266,500	256,600	10,000	541,677	766,277	-224,600
50	200	50	522,750	512,750	10,000	1,052,952	1,532,552	-479,600
100	200	50	1,035,300	1,015,300	20,000	2,085,452	3,035,052	-949,600

Once again, we modify constraint (4.4) to integrate the new variable through:

$$\sum_{m \in \mathcal{N}} \sum_{(i,j) \in \mathcal{A}} \sum_{c \in \mathcal{C}} R_{ij}^{c} \alpha(t_{ij}^{m}) h_{ij}^{mc} \leq \theta \tag{4.22}$$

The remainder of the model stays the same, accommodating h_{ij}^{mc} where needed. This SLPIL model obtains the same solution as SLP. Moreover, through extensive experiments, we have shown that SLPIP converges to a solution more rapidly than SLP (more in Section 4.3). The complete formulation of the model can be found in Appendix C.

Finally, we can easily adapt SLPIL, as well as SLP, the MCN formulation outlined in Section 3.6. In order to do so, we remove Eqn. (4.7) and substitute Eqn. (4.4) with Eqn. (3.30) and make the necessary changes in the remainder of the model.

4.2 A Two-Stage Heuristic Algorithm

By design, the problem is composed of two main aspects: Hazmat Transportation Network Design and the location of Hazmat Response Team on nodes to further reduce risk. Because both are combined within a single problem to obtain the best possible network and emergency response, the network design and HRT locations are determined simultaneously. This results in a complex problem that uses a high number of variables to represent the interaction of all the factors, further exacerbated by the linearization needed. While assessing both problem aspects at once yields a global optimal solution, it is computationally slow to do so. Additionally, the problem size increases considerably and leads to substantially longer solution times; this approach is thus not applicable for large-scale problems.

The goal of the heuristic algorithm we developed, which we refer to as **HM**, is a solution method that is computationally faster, while maintaining a certain objective function accuracy, yielding a solution that is as close as possible to the the optimal solution (which can be obtained with the single-level reformulation method outlined above) in a considerably lower time.

We propose an approach that divides the problem into its two main features, resulting in a first problem that tackles the hazmat network transportation network design and a second one that focuses on the location of emergency response teams to improve the risk profile of the network. These are solved sequentially, as the network designed in the first phase becomes the network on which the HRT are optimally placed; furthermore, the first problem yields the shortest paths of the carriers.

Because the problem is now broken into two parts, no linearization is needed, further contributing to improving the solution time. However, the first problem is solved optimally without taking into account the following model, thus limiting its solution and not guaranteeing an optimal solution to the problem. Numerous tests, however, have proven the approach to be an effective method, yielding results often close to optimal, as outlined in Section 4.3. More details regarding the algorithm and the problems are given below.

4.2.1 Algorithm

First, we must identify all the road links that could satisfy both the best and worst response time requirements. For each arc, the following equations are used:

$$\min\{t_{ij}^{m\gamma} | \forall m \in \mathcal{N}\} \leq T_{best} \tag{4.23}$$

$$\min\{t_{ij}^{m\beta} | \forall m \in \mathcal{N}\} \leq T_{worst} \tag{4.24}$$

If either of those conditions is not satisfied, response time cannot be guaranteed to be within the desired service level and link (i, j) must be set to be unavailable ($y_{ij} = 0$). To do this, a new variable $\lambda_{ij} \in \{0, 1\}$, where $\lambda_{ij} = 0$ if the link (i, j) cannot be covered by any emergency response team and 1 otherwise, is introduced. The λ_{ij} values are calculated before solving the problem. The condition $y_{ij} \leq \lambda_{ij}$ is then added to ensure that a road link can only be considered for the transportation of hazmat if it can be reached in a timely manner.

This step is implicitly part of the single-level formulation, as links that cannot be covered will not be made available for the transportation of hazmat. That step must be

explicitly done within the heuristic method, as the information regarding which arcs are within an acceptable response time of a potential HRT location is found in the second problem, but is needed in the first one.

Subsequently, the two problems are defined: (1) design of hazmat transportation network and carrier routing, and (2) location of HRT on the network defined. The problems are solved successively and in order, as the solution to the first problem defines the constraint of the second one.

We denote the solutions of the first and second problem as w^* and z^* respectively, observing that $w^* \geq z^*$, as emergency response teams can only make the risk assessment more robust and reduce the total risk on the network, as the worst response time possible is assumed for all links the first problem. The procedure used is summarized in Algorithm 1.

Algorithm 1 Two-Stage Heuristic Algorithm

Step 1: Identify links that cannot be covered by any HRT at any location

for $(i,j) \in \mathcal{A}$ **do**

if $\min\{t_{ij}^{m\gamma} | \forall m \in \mathcal{N}\} \leq T_{best} \wedge \min\{t_{ij}^{m\beta} | \forall m \in \mathcal{N}\} \leq T_{worst}$ **then**

Link within acceptable response time of potential HRT location, set $\lambda_{ij} = 1$

else

Link cannot be covered, set $\lambda_{ij} = 0$

Step 2: Solve the HTND problem (problem 1 - HM.1)

Optimal solution: $w^*(x_{ij}^{c*}, y_{ij}^*)$

Step 3: Solve the HRT location problem (problem 2 - HM.2)

Set the available road links $y_{ij} \leftarrow y_{ij}^*$

Set routing of the hazmat shipments $x_{ij}^c \leftarrow x_{ij}^{c*}$

Optimal solution: $z^*(v^{m*}, h_{ij}^{m*})$

Optimal solution of complete problem: z^*, with optimal values $x_{ij}^{c*}, y_{ij}^*, v^{m*}, h_{ij}^{m*}$

First-Stage Problem (HM.1)

This problem focuses on designing the hazmat transportation network and the routes used by the carriers, without taking into account any emergency response or requiring service levels to be met with given probabilities. Because risk is ultimately decided by the carriers' routing, a min max expression is required to ensure the pessimistic formulation of the problem; the same min max expression is adopted. HM.1 is formulated as follows:

$$\min \quad w \tag{4.25}$$

$$\text{s.t.} \quad \sum_{m\in\mathcal{N}} \sum_{(i,j)\in\mathcal{A}} \sum_{c\in\mathcal{C}} R_{ij}^c x_{ij}^c \leq \theta \tag{4.26}$$

$$y_{ij} = y_{ji} \qquad \forall (i,j) \in \mathcal{A} \tag{4.27}$$

$$\sum_{i\in\mathcal{N}:(i,j)\in\mathcal{A}} x_{ij}^c - \sum_{i\in\mathcal{N}:(i,j)\in\mathcal{A}} x_{ji}^c = \begin{cases} 1 & j = o^c \\ -1 & j = d^c \\ 0 & \text{otherwise} \end{cases} \qquad \forall j \in \mathcal{N}, \forall c \in \mathcal{C} \tag{4.28}$$

$$x_{ij}^c \leq y_{ij} \qquad \forall (i,j) \in \mathcal{A}, \forall c \in \mathcal{C} \tag{4.29}$$

$$\pi_j^c - \pi_i^c \leq n^c l_{ij} + M(1 - y_{ij}) \qquad \forall (i,j) \in \mathcal{A}, \forall c \in \mathcal{C} \tag{4.30}$$

$$\pi_{d^c}^c - \pi_{o^c}^c \geq \sum_{(i,j)\in\mathcal{A}} n^c l_{ij} x_{ij}^c \qquad \forall c \in \mathcal{C} \tag{4.31}$$

$$y_{ij} \leq \lambda_{ij} \qquad \forall (i,j) \in \mathcal{A} \tag{4.32}$$

$$x_{ij}^c \in \{1,0\}, y_{ij} \in \{1,0\} \tag{4.33}$$

$$\pi^c \text{ free} \tag{4.34}$$

This is built around the single-level model, without any linearization. All features related to the location of HRT are removed, including deletion of the Response Time Factor to assess risk, resulting in the total risk being measured solely according to R_{ij}^c (constraint (4.26)). Additionally, constraint (4.32) is included to ensure that the network designed contains only road links that can be covered by emergency response teams in the subsequent problem; otherwise the problem would have no solution.

Second-Stage Problem (HM.2)

The second problem deals with locating the emergency response teams on the network designed in the previous step, and assigning their coverage to the various available road links. The optimal carrier routes (shortest path) have already been decided through the solution obtained in the earlier step, and therefore the variables y_{ij} and x_{ij}^c become constants in this stage, resulting in a computationally fast problem to solve.

The usual constraints for the arc coverage problem and uncertainty apply, resulting in the following formulation HM.2:

$$\min \quad z = \sum_{m \in \mathcal{N}} \sum_{(i,j) \in \mathcal{A}} \sum_{c \in \mathcal{C}} R_{ij}^c \alpha(t_{ij}^m) h_{ij}^m x_{ij}^{c*} \tag{4.35}$$

$$\text{s.t.} \quad \sum_{m \in N} v^m \leq H \tag{4.36}$$

$$h_{ij}^m \leq v^m \qquad \forall (i,j) \in \mathcal{A}, \forall m \in \mathcal{N} \tag{4.37}$$

$$\sum_{m \in N} h_{ij}^m \geq x_{ij}^{c*} \qquad \forall (i,j) \in \mathcal{A}, \forall c \in \mathcal{C} \tag{4.38}$$

$$\sum_{m \in N} h_{ij}^m \leq 1 \qquad \forall (i,j) \in \mathcal{A} \tag{4.39}$$

$$P(T_{ij}^m h_{ij}^m \leq T_{best}) \geq 1 - \gamma \qquad \forall (i,j) \in \mathcal{A}, \forall m \in \mathcal{N} \tag{4.40}$$

$$P(T_{ij}^m h_{ij}^m \leq T_{worst}) \geq 1 - \beta \qquad \forall (i,j) \in \mathcal{A}, \forall m \in \mathcal{N} \tag{4.41}$$

$$v^m \in \{1,0\}, h_{ij}^m \in \{1,0\} \tag{4.42}$$

Table 4.3 compares the problem sizes of the SLPIL and the heuristic method. We can observe that all the variables are the same, except for h, resulting in a difference of $|N| \times |A| \times (|C|-1)$[1] variables between SLPIL and the heuristic algorithm, with the latter having fewer variables and a noticeably smaller number of constraints. Additionally, Table 4.4 shows some examples of problem sizes for different networks and shipment quantities. We can clearly see the that SLPIL does not fare well with increased problem sizes, whereas

[1]Variable h, last row of Table 4.3

the HM scales much better with bigger networks and increased number of shipments, due to the fact that two smaller problems are solved.

Finally, with respect to MCN model, HM can be easily revised with the appropriate constraints by updating the formulation with Eqn. (3.30). The algorithm must be updated by removing Step 1 in Algorithm 1 to incorporate all the links within the model.

Table 4.3: Problem Size Comparison of SLPIL & Heuristic Algorithm

Variable	SLPIL (Index: Amount)	HM (Index: Amount)	
		HM.1	HM.2
x	$c,(i,j):\|\mathcal{C}\|\times\|\mathcal{A}\|$	$c,(i,j):\|\mathcal{C}\|\times\|\mathcal{A}\|$	
y	$(i,j):\|\mathcal{A}\|$	$(i,j):\|\mathcal{A}\|$	
π	$c,j:\|\mathcal{C}\|\times\|\mathcal{N}\|$	$c,j:\|\mathcal{C}\|\times\|\mathcal{N}\|$	
v	$m:\|\mathcal{N}\|$	-	$m:\|\mathcal{N}\|$
h	$m,c,(i,j):\|\mathcal{N}\|\times\|\mathcal{C}\|\times\|\mathcal{A}\|$	-	$m,(i,j):\|\mathcal{N}\|\times\|\mathcal{A}\|$

Table 4.4: Problem Size Comparison of SLPIL & Heuristic Algorithm - Example

Set Size			Number of Variables					Number of Constraints				
				Heuristic					Heuristic			
$\|\mathcal{N}\|$	$\|\mathcal{A}\|$	$\|\mathcal{C}\|$	SLPIL	HM.1	HM.2	Total	Diff	SLPIL	HM.1	HM.2	Total	Diff
25	100	10	26,375	1,350	2,252,	3,875	22,500	78,262	2,362	7,701	10,063	68,199
25	100	25	65,750	3,225	2,525	8,875	60,000	195,652	5,752	7,701	13,453	182,199
25	100	50	131,375	6,350	2,525	8,875	122,500	391,302	11,402	7,701	19,103	372,199
50	200	10	102,750	2,700	10,050	12,750	90,000	306,512	4,712	30,401	35,113	271,399
50	200	25	256,600	6,450	10,050	16,500	240,000	766,277	11,477	30,401	41,878	724,399
50	200	50	512,750	12,700	10,050	22,750	490,000	1,532,552	22,752	30,401	53,153	1,479,399
100	200	50	1,015,300	15,200	20,100	33,300	980,000	3,035,052	25,252	60,401	85,653	2,949,399

4.3 Computational Results

Let us contrast the performance of the different solution methods we propose on a random network. A comparison of the SLP and SLPIL shows that both lead to an exact solution,

but the improved linearization reduces the solution time. We then evaluate SLPIL and HM to asses the accuracy of the two-stage heuristic algorithm and its computational time improvement.

Because the results of the different methodologies are dependent upon the transportation network upon which the problem is based, we solve each problem instance on a randomized network. These problem instances that we use to compare the different algorithms remove the network type as a factor. We decide on a number of nodes, and then specify the probability that an arc exists between any 2 nodes in the network to represent the number of road links. An expanded number of links will enable a better understanding of performance on increasingly larger networks. Additionally, we randomize the shipments in terms of origin-destination pair, using network nodes and type of hazmat each was transporting; these are increased to assess the impact the number of shipments has on the optimal risk. Ten problem instances (N=10) are computed for each nodes-link probability-shipments combination[2].

We examine the computation time (s) and optimal risk, calculating the Mean Percentage Difference (MPD) between two methods with $\frac{1}{N}\sum_{n=1}^{N}\frac{SLP_n - SLPIL_n}{SLPIL_n} \times 100\%$ for SLP-SLPIL and $\frac{1}{N}\sum_{n=1}^{N}\frac{SLPIL_n - HM_n}{HM_n} \times 100\%$ for SLPIL-HM, as well as the solution gap, in terms of percentage point differences between the algorithms evaluated. Note that the solution time for each problem is limited to 2 hours (7200s), and a 5% solution gap is applied.

For the computation, Python 3.9 and Gurobi (gurobipy 9.1.1) is used to develop the algorithms and solve the problems. A 6-core processor (AMD Ryzen 3600X) and 16 GB of RAM are used.

[2]The following parameters are used: $H = |N|/2$, $T_{best} = 30$, $T_{worst} = 60$, $\beta, \gamma = 0.5, 0.8$, $var = 0.25t_{ij}^{m}$. A normal distribution is used to model the response time.

SLP vs SLPIL

Table 4.5 compares performance of the the SLP and SLPIL methods, showing the average solution's computational time and objective for each network and shipment combination. Various network sizes are used, with 10 and 30 nodes each with a link probability of 0.2, 0.5 and 0.8, as well as 10 and 30 unique origin-destination shipments; 10 instances are completed on random networks and shipment sets for each., for a total of 180 instances. The solutions are examined for these problem sizes, as beyond that SLP cannot obtain an optimal solution within 2 hours.

Table 4.5: Solution Comparison of SLP and SLPIL

Problem Size			Computation Time (s)			Gap			Optimal Risk		
$\|\mathcal{N}\|$	link prob ($\|\mathcal{A}\|$)	$\|\mathcal{C}\|$	SLP	SLPIL	MPD	SLP	SLPIL	Difference[3]	SLP	SLPIL	MPD
10	0.2 (17)	10	0.08	0.02	180.1%	0.0%	0.0%	0	32.6	32.6	0.0%
		20	0.09	0.03	77.1%	0.0%	0.0%	0	45.7	45.7	0.0%
		50	1.41	0.29	203.9%	0.0%	0.0%	0	100.5	100.5	0.0%
		80	2.59	0.59	167.2%	0.0%	0.0%	0	103.0	103.0	0.0%
	0.5 (43)	10	3.07	0.27	1,077.1%	0.0%	0.0%	0	7.9	7.9	0.0%
		20	7.38	0.94	849.3%	0.0%	0.0%	0	24.5	24.5	0.0%
		50	59.19	7.63	839.2%	0.0%	0.0%	0	55.6	55.6	0.0%
		80	603.77	66.35	730.1%	0.0%	0.0%	0	89.7	89.7	0.0%
	0.8 (74)	10	6.91	0.59	1,611.4%	0.0%	0.0%	0	4.5	4.5	0.0%
		20	73.66	9.81	877.4%	0.0%	0.0%	0	9.7	9.7	0.0%
		50	1,209.13	194.04	776.9%	0.0%	0.0%	0	27.0	27.0	0.0%
		80	4,379.87	697.99	547.9%	1.1%	0.0%	0	39.7	39.6	0.2%
30	0.2 (178)	10	86.67	5.93	1,572.9%	0.0%	0.0%	0	8.5	8.5	0.0%
		20	469.37	61.30	660.4%	0.0%	0.0%	0	19.5	19.5	0.0%
	0.5 (438)	10	1,121.76	34.03	5,202.1%	0.0%	0.0%	0	4.4	4.4	0.0%
		20	7,069.71	687.70	1,842.7%	17.8%	0.0%	17.8	8.3	7.2	15.1%
	0.8 (696)	10	5,429.00	104.37	8,890.7%	9.7%	0.0%	9.7	2.4	2.3	2.9%
		20	7200.64	1227.15	493.8%	96.1%	0.0%	96.1	16.6	3.3	447.4%

As we can see, SLPIL is much faster computationally as it can solve the same problem in a much shorter time than SLP, with the latter notably taking from 5 to 90 times longer than SLPIL. Perhaps more importantly, the solutions obtained from the two methods

are identical[3], except when SLP method cannot finish within the maximum allowed time. Consider the case of 30 nodes, 20 shipments, and 0.5 and 0.8 link probability, where the solution obtained was inevitably sub-optimal within the time limit. Additionally, we can see that the gap for SLP increases as a problem's computational time approaches 2 hours (reaching an average of 96% for the last problem instance), while SLPIL attains a 0% gap for those instances.

SLPIL vs HM

The Heuristic Method solution time is calculated by adding the computation time of the first and second problem ($SolTime(HM) = SolTime(HM.1) + SolTime(HM.2)$). The solution of the overall algorithm is equal to the optimal solution obtained in the second problem ($HM^* = HM.2^*$, where * denotes the optimal objective function value).

Table 4.6 compares the performance of the SLPIL and HM methods in terms of computation time and solution accuracy. Per design, the heuristic solution is much faster than the single-level reformulation method as shown in the "Computation Time (s)" columns, with SLPIL taking as much as 450 times as long as HM (e.g. 100 nodes, 0.5 link prob, 10 shipments). Some problem sizes resulted in neither approach being able to reach an optimal solution within 2 hours (as in 30 nodes, 0.8 link prob, 50 shipments and 50 nodes, 0.5 link prob, 50 shipments). For such cases, HM resulted in a much lower gap (90.8% vs 5.2% and 93.9% vs 11.1%). Similar to SLP, as the problems grow bigger, the gap increases after the maximum allowed time is reached; HM's maximum gap is 11% (on the most time consuming problem size) and generally does not go above 5% (the gap allowed for the computation).

Additionally, we compare the solutions obtained with both methods on the same problems. As expected, because of the locally optimal solutions of the HM algorithm problems, the risk profile obtained by SLPIL is lower. The inverse is true whenever SLPIL cannot reach an optimal solution within the time limit, as HM converges more quickly to a solu-

[3]There can be slight discrepancies, for the example with 30 nodes, 0.8 link prob and 10 shipments, there is a difference of 0.01. That is an acceptable error, due to the 5% gap imposed and other approximations.

Table 4.6: Solution Comparison of SLPIL and HM

Problem Size			Computation Time (s)			Gap			Optimal Risk		
$\|\mathcal{N}\|$	link prob ($\|\mathcal{A}\|$)	$\|\mathcal{C}\|$	SLPIL	HM	MPD	SLPIL	HM	Difference	SLPIL	HM	MPD
10	0.2 (17)	10	0.02	0.01	54.8%	0.0%	0.0%	0	32.6	32.6	0%
		20	0.04	0.01	154.0%	0.0%	0.0%	0	45.7	46.3	-1.6%
		50	0.29	0.08	519.1%	0.0%	0.0%	0	100.5	101.3	-0.7%
		80	0.6	0.11	294.5%	0.0%	0.0%	0	103.0	103.6	-0.5%
	0.5 (43)	10	0.27	0.08	248.2%	0.0%	0.0%	0	7.9	8.4	-6.6%
		20	0.94	0.26	209.5%	0.0%	0.0%	0	24.5	25.9	-4.7%
		50	7.64	2.13	251.5%	0.0%	0.0%	0	55.6	58.6	-5.1%
		80	66.35	11.99	533.3%	0.0%	0.0%	0	89.7	97.7	-8.7%
	0.8 (74)	10	0.59	0.13	464.4%	0.0%	0.0%	0	4.5	5.3	-14.1%
		20	9.82	1.25	863.0%	0.0%	0.0%	0	9.7	10.5	-8.5%
		50	194.05	65.01	525.8%	0.0%	0.0%	0	27.0	29.2	-8.4%
		80	698	244.4	300.9%	0.0%	0.0%	0	39.6	44.3	-10.0%
30	0.2 (175)	10	5.93	0.26	2,857.8%	0.0%	0.0%	0	8.5	9.3	-10.9%
		20	61.3	2.82	5,141.7%	0.0%	0.0%	0	19.5	23.0	-13.0%
		50	2,425.87	905.37	1,052.8%	0.3%	0.0%	0	58.9	65.4	-9.7%
		80	6,082.43	2747.19	841.9%	38.9%	5.6%	0	194.7	106.2	120.4%
	0.5 (438)	10	34.03	1.15	4,137.5%	0.0%	0.0%	0	4.4	5.1	-11.4%
		20	687.7	13.39	6,443.6%	0.0%	0.0%	0	7.2	8.5	-15.7%
		50	7,201.22	2,729.45	1,217.4%	90.8%	5.2%	0	225.9	26.1	789.8%
	0.8 (702)	10	104.37	1.37	15,309.3%	0.0%	0.0%	0	2.3	2.6	-9.3%
		20	1,227.16	741.74	19,456.7%	0.0%	0.5%	-0.5	3.3	3.9	-12.6%
		50	7,200.69	7,200.36	0%	75.9%	7.6%	63.8	38.1	11.4	233.39%
50	0.2 (489)	20	825.05	3.34	34,004.9%	0.6%	1.9%	-1.3	13.3	15.6	-14.3%
		50	6,061.57	1,791.21	1,689.7%	62.7%	4.4%	58.3	285.5	41.9	616.7%
	0.5 (1222)	20	2,572.67	23.27	30,201.5%	1.9%	2.3%	-0.4	3.3	3.9	-13.1%
		50	7,218.75	7,200.52	0.2%	93.9%	11.1%	82.8	180.9	13.8	1,206.3%
	0.8 (1958)	20	3,531.28	42.62	8,569.6%	41.2%	3.0%	38.2	33.1	3.3	782.9%
100	0.1 (985)	10	671.37	1.44	56,600.2%	0.3%	0.4%	-0.1	6.9	8.1	-13.4%
		20	615.12	63.12	1,242.8%	0.6%	1.3%	-0.7	10.3	11.9	-12.4%
	0.2 (2009)	10	224.39	3.43	8,501.6%	0.2%	0.5%	-0.3	2.4	3.1	-21.3%
		20	-	103.30	-	-	1.1%	-	-	8.9	-
	0.5 (4974)	10	-	45.02	-	-	0.28%	- -	-	0.5	-
		20	-	172.64	-	-	1.3%	-	-	2.2	-
150	0.1 (2233)	10	-	6.42	-	-	0.5%	-	-	4.8	-
		20	-	148.05	-	-	0.6%	-	-	2.9	
200	0.1 (3963)	10	-	12.83	-	-	0.2%	-	-	4.0	-
		20	-	545.65	-	-	0.2%	-	-	8.4	-

tion, and the solution obtained results in a lower risk [4]. SLP results in solutions with up to about 20% overall risk.

[4]This might not be obvious when looking at the table as the average values are presented. For example, with 50 nodes, 0.8 link prob, and 20 shipments, there were 6 problems that completed within 2 hours, while the rest did not. This resulted, on average, in a higher risk solution for SLPIL.

The last part of the table shows the computational results for problems using HM alone, as SLPIL would not complete within 2 hours for any of the problems proposed. As we can see, the heuristic solution method proposed is still effective for large problems, as it can solve a problem having 200 nodes, $\sim$4000 links and 20 shipments in under 600 seconds. Problems of larger sizes could not be evaluated because of memory issues, as the problems examined would not fit within the available memory.

More broadly, we can observe that, generally, for the same number of shipments, a larger network (more nodes, higher link probability) will result in a lower risk caused by the carriers. Intuitively, this can be explained by the fact that there are more possible routes for the shipments to take, and more HRT candidate locations to cover the road links. Unsurprisingly, the number of shipments is the factor that most affects the risk, as more shipments will inevitably lead to more risk. Additionally, the number of shipments appears to be the factor having the greatest impact on performance time, with the computation time increasing notably within the same network size.

Chapter 5

Case Study

Here we present a case study, where we apply one of the two proposed models to a real transportation network in Southeast China. We examine the performance of the SLPIL algorithm outlined in Chapter 4, compare the risk obtained against different risk measurement approaches and other risk-mitigation mechanisms, and perform an analysis on some of the key factors that may be variable, and the effect of those changes.

5.1 Network Structure and Data Estimation

The real-world highway transportation network of the city of Nanchang in the Jiangxi Province in China is utilized to conduct our case study. The network has a total of 32 nodes and 102 directed arcs (Figure 5.1), with lengths ranging from 7 km to 35 km, calculated according to the distance between the nodes.

There are two objectives within the proposed model to account for the decisions of the government's agency and the carriers: the risk throughout the network, calculated according to Eqn. (4.4), and the carrier's travel distance, determined by the arcs chosen and their length. We next present the details of the estimation of parameter data.

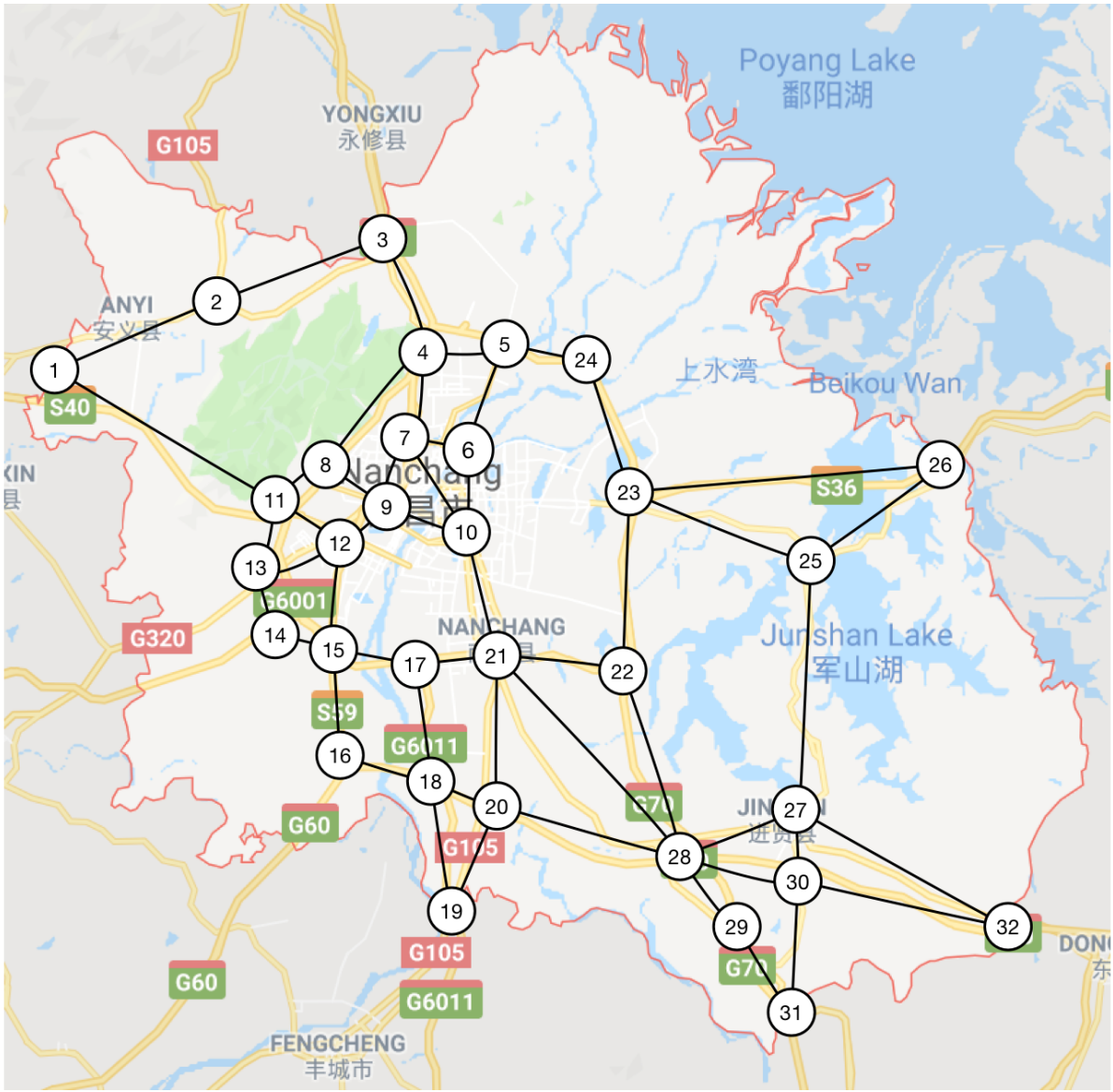

Figure 5.1: Nanchang Network (Ke et al., 2020)

5.1.1 Distance

The length of each road link is obtained according to the distance between two nodes on the Nanchang transportation network (in km) (Ke et al., 2020). The carrier's objective is

then determined by the total length of arcs chosen for the transportation of hazmat from o^c to d^c.

5.1.2 Risk

As discussed in Chapter 3, we compute the risk based on 1) population exposure of the surrounding area, 2) incident rate of a certain link, and 3) hazmat release rate, given an incident.

The population density was obtained from the 2010 China Population Census by the National Bureau of Statistics of China. The population exposure is then obtained by integratively considering the population density for each road link and the impact radius of the corresponding hazmat type (Table 5.1).

For the incident rate, we randomize it with reference to the 20-year survey data from 1997 to 2016 in the Large Truck and Bus Crash Facts 2016 (Federal Motor Carrier Safety Administration, 2018). To be specific, the rate range is computed as between the highest and lowest total rate of large trucks involved in fatal, injury, and property-only crashes per 100 million vehicle miles traveled, i.e., 2.34×10^{-6} (1999 data) and 0.96×10^{-6} (2010 data).

Additionally, three hazmat types ($\mathcal{K}$), with the corresponding risk profiles, are considered. We specify the three types of hazmat types as liquid, gaseous, and solid (Ke et al., 2020). Because of the different properties, these hazmats have distinct release rates, which are summarized in Table 5.1.

Table 5.1: Hazmat Types, $k \in \mathcal{K}$

k	Hazmat Type	Release Rate	Exposure Radius (km)
1	solid	0.091	0.5
2	gas	0.072	0.8
3	liquid	0.187	1.6

Based on the previous estimates, the risk distribution of this network can be illustrated in Figure 5.2.

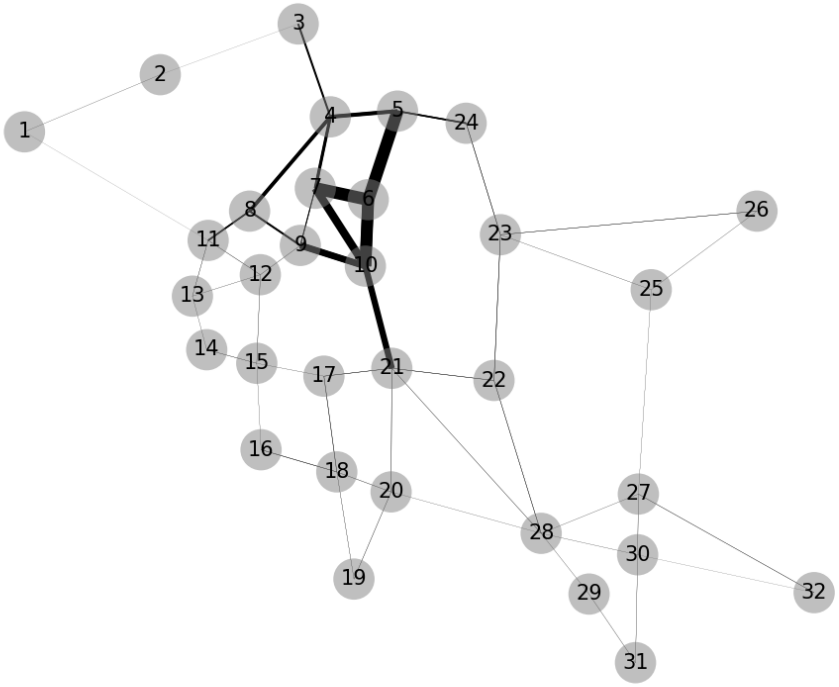

Figure 5.2: Distribution of Risk of Nanchang Network

5.1.3 Time

The length of an arc is constant, yet we allow for variations in response time for emergency response teams, as the HRT may travel at a faster speed than the speed limit, or at a slower speed when traffic or other undesired conditions may exist. Any relevant probability

distribution could be applied to model the travel time from one location to another. We herein assume a normally distributed variable, T_{ij}^m with a distribution $T_{ij}^m \sim \mathrm{N}(\mathrm{t}_{ij}^m, \sigma^2)$, with t_{ij}^m being the average time to fully cover link (i, j) from node m (where HRT is located), which can be defined as:

$$t_{ij}^m = t_{ij} + \min(t_{mj}, t_{mi}) \qquad \forall (i,j) \in \mathcal{A}, \forall m \in \mathbf{N} \tag{5.1}$$

where t_{ij} is the travel time to reach node j from node i. The average travel time of each link is calculated by dividing the link length by the speed limit (given by the Implementation Regulations of the People's Republic of China Road Traffic Safety Law (`http://www.cnca.gov.cn/bsdt/ywzl/flyzcyj/zcfg/201707/t20170711_54697.shtml`)). The optimistic and pessimistic service level constraints (3.11) and (3.12) can be then written as:

$$(\sigma z_{(\gamma)} + t_{ij}^m) h_{ij}^m \leq T_{best} \qquad \forall (i,j) \in \mathcal{A}, \forall m \in \mathbf{N} \tag{5.2}$$

$$(\sigma z_{(\beta)} + t_{ij}^m) h_{ij}^m \leq T_{worst} \qquad \forall (i,j) \in \mathcal{A}, \forall m \in \mathbf{N} \tag{5.3}$$

with z being the z-value of the standard normal distribution. Moreover, defining $(\sigma z_{(\gamma)} + t_{ij}^m)$ as $t_{ij}^{m\gamma}$ for the best case scenario (optimistic) and $(\sigma z_{(\beta)} + t_{ij}^m)$ as $t_{ij}^{m\beta}$ for the worst one (pessimistic) Eqns. (5.2) and (5.3) can be written as:

$$t_{ij}^{m\gamma} h_{ij}^m \leq T_{best} \qquad \forall (i,j) \in \mathcal{A}, \forall m \in \mathbf{N} \tag{5.4}$$

$$t_{ij}^{m\beta} h_{ij}^m \leq T_{worst} \qquad \forall (i,j) \in \mathcal{A}, \forall m \in \mathbf{N} \tag{5.5}$$

The variance of the travel time is defined as $(\sigma_{ij}^m)^2 = \eta t_{ij}^m$, i.e., a percentage of the average travel time of the link examined, where η is a variance percentage factor, assumed constant for all links in the network. This is applied to Eqns. (5.2) and (5.3) to find $t_{ij}^{m\gamma}$ and $t_{ij}^{m\beta}$. Also, we set $T_{best} = 25$ min and $T_{worst} = 50$ min for the base case.

Finally, the probabilities that the random variable is within the pre-defined values affect the service levels required. We adopt $\gamma = 80\%$ and $\beta = 90\%$ for the optimistic and pessimistic response times respectively to describe the service levels in the base case.

5.1.4 Response Time Factor (RTF)

A key aspect of the risk assessment we use here is the inclusion of the response time from an HRT to an accident location to reduce the spread of hazardous materials. Naturally, the

faster the response, the lesser the extent of the damage around the incident site. Different approaches can be taken to represent the relationship between response time and risk and we do so through a Response Time Factor (RTF), earlier defined as $\alpha(t_{ij}^m)$.

Following the extensive research outlined in Transportation Research Board and National Academies of Sciences, Engineering, and Medicine (2011), we adopt the same RTF. This is a discrete scale that assigns a value according to whether the response time t_{ij}^m is within a certain factor of the desired response time, here defined as T_{best}. Table 5.2 outlines the RTF, depending on the value of t_{ij}^m with respect to T_{best}.

Table 5.2: Response Time Factor, adapted from the Transportation Research Board and National Academies of Sciences, Engineering, and Medicine (2011)

RTF $\alpha(t_{ij}^m)$	Description
1	Response time meets or exceed the desired response time, i.e. $t_{ij}^m \leq T_{best}$
2	Response time is within 125% of the desired response time, i.e. $t_{ij}^m \leq 1.25T_{best}$
3	Response time is within 150% of the desired response time, i.e. $t_{ij}^m \leq 1.5T_{best}$
4	Response time is within 200% of the desired response time, i.e. $t_{ij}^m \leq 2T_{best}$
5	Response time is more that double the desired response time, i.e. $t_{ij}^m > 2T_{best}$

5.1.5 Other data

Table 5.3 summarizes the parameter values used in our base case. The values chosen represent solutions to average case scenarios for the Nanchang network; a sensitivity analysis around some of these parameters is explored later in this chapter.

Furthermore, we establish a sample shipment set of size 10, whose features are summarized in Table 5.4. This was designed to provide origin-destination pairs of shipments that are spread out across the network, and a diverse number of trucks per shipment and hazmat types being transported. This shipment set is used to compare the effect of different factors on the solution obtained by the model. However, other random shipment sets are used to compare the effect of different shipment sizes.

Table 5.3: Summary of Base Parameters

Parameter	Value
Hazmat demand ($\|\mathcal{C}\|$)	10
Number of hazmat types ($\|\mathcal{K}\|$)	3
Hazmat shipment size (n)	1 to 10
Max number of HRT (H)	5
γ, β	80%, 90%
η, such at $(\sigma_{ij}^m)^2 = \eta t_{ij}^m$	0.25
T_{best}, T_{worst} (min)	25, 50

Table 5.4: Sample Shipment Set

Shipment (c)	Origin-Destination (o^c, d^c)	Size of Shipment (n^c)	Hazmat Type (k)
1	(2,29)	7	1
2	(4,20)	2	2
3	(7,22)	9	3
4	(8,19)	4	2
5	(6,32)	3	2
6	(10,26)	1	3
7	(31,12)	8	1
8	(27,3)	9	2
9	(16,23)	6	1
10	(25,9)	8	1

5.2 Algorithm Performance

We choose the SLPIL model (i.e. the exact method with best-performing formulation) (Section 4.1.2) as it is the model that provides the most accurate results in the lowest time for the given problem size, well below the 2 hour time limit. This further cements this method as a practical solution approach for real transportation networks.

The hazmat demand (number of carriers) is randomized. We optimize the model for 10, 30, 50, 75, 100, 150, 200, and 300 unique shipments ($\mathcal{C}$), solving 20 instances for each. The average computation time, risk, and gap (for MCV) are summarized in Table 5.5.

MCN can be solved in similar time ranges and results in similar risks, and therefore that information is omitted.

Table 5.5: SLPIL Basic Performance on Nanchang Network

Number of Shipments $\lvert\mathcal{C}\rvert$	CPU Time (s)	Gap (%)	Max System Risk θ
10	0.5	0.0	1.6
30	5.9	0.0	6.8
50	25.4	0.0	10.9
75	75.9	0.0	17.0
100	93.5	0.0	24.3
150	257.8	0.0	35.3
200	1,197	0.0	50.7
300	3,406	0.0	74.6

It is clear that SLPIL (Single-Level Problem Improved Linearization) can reach an optimal solution in a very short time, up to a maximum average of 3,406s for 300 shipments, with a consistent gap of zero. This result shows that the proposed solution proposed is applicable for real-world problems with a considerable number of shipments. Naturally, from Table 5.5, we can also observe that the increased number of shipments leads to higher total risk on the network. This is simply because the number of shipments directly contributes to the increased risk of the network.

To further show the impact of shipment numbers, we introduce Figure 5.3, which depicts the normalized computation time per shipment, i.e.,

$$\frac{\text{CPU Time}}{|\mathcal{C}|}.$$

We can see that the variation within each category considerably increases with the number of shipments. This would imply that SLPIL is not applicable when there is an extremely high number of shipments. A similar observation was made in Section 4 when comparing the different solution methodologies.

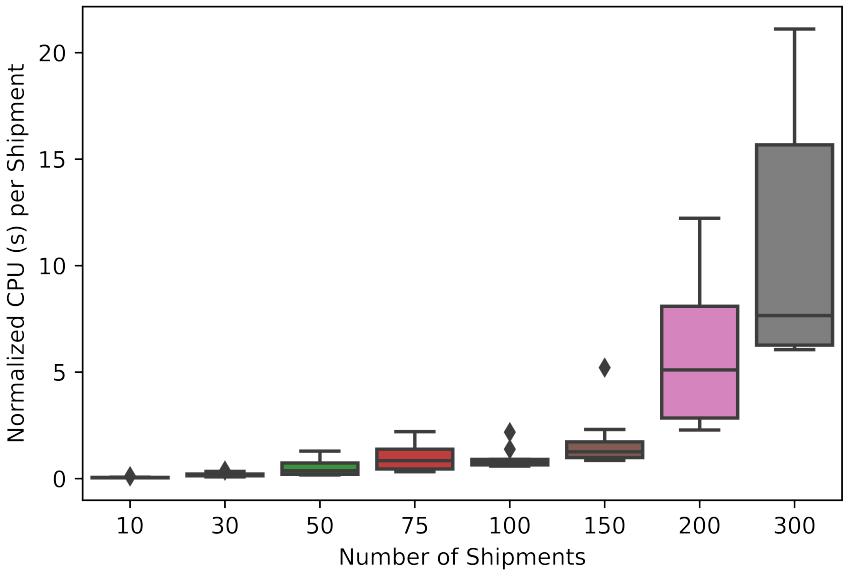

Figure 5.3: Normalized CPU per shipment

5.3 Performance Comparison of MCV and MCN

The MCV and MCN models have a very similar structure. However, their objectives differ, as MCV prioritizes the coverage of all the links that can potentially be used for the transportation of hazardous materials, whereas MCN relaxes that constraint by allowing some network arcs to be available, despite the fact that their coverage requirements cannot be satisfied.

By applying both models to the Nanchang network, given the shipment set of Table 5.4, we can see that MCV has both a higher total network risk ($\theta = 1.61$) and carriers' distance (1,144 km), while MCN results in lower overall risk ($\theta = 1.53$) and carriers' distance (1,077 km), as noted in Table 5.6. The difference in risk, however, comes at the cost of link coverage.

For a comprehensive comparison, we define four indicators as follows.

Table 5.6: Comparison of Results: MCV & MCN (5 HRTs)

Model	θ	Carriers Distance	CN	CV	CVA	CVU	HRT Locations
MCV	1.61	1,144	60.8%	72.5%	120.4%	100.%	[1, 3, 17, 23, 30]
MCN	1.53	1,077	66.7%	62.7%	94.1%	97.5%	[1, 3, 12, 23, 28]

Connectivity Measure (CN) computed as

$$CN = \frac{\text{\# opened links}}{\text{\# total links}}$$

Coverage Measure (CV) measured by

$$CV = \frac{\text{\# covered links}}{\text{\# total links}}$$

Percentage of Available Links Being Covered (CVA) evaluated as

$$CVA = \frac{\text{\# covered links}}{\text{\# available links}}$$

Percentage of Used Links Being Covered (CVU) coverage used links, measured as

$$CVU = \frac{\text{\# links used and covered}}{\text{\# available links}}$$

Referring to Table 5.6, and Figures 5.4 and 5.5, MCN offers a higher CN with 66.7% (68/102) of all links being available for the transportation of hazmat, against 60.8% (45/102) for MCV. However, MCV, by design, has a higher CV with a value of 72.5% against 62.7% for MCN. Additionally, the coverage of available links, more important to assess the capabilities in responding to potential accidents, is noticeably different. MCN only covers 94.1% (64/68) of all the available links, with links [(18, 19), (19, 18), (19, 20), (20, 19)] being open but uncovered. On the other hand, MCV has a coverage rate of 120.4%. The coverage for MCV is above 100%, as the model offers coverage of links that are not open for the transportation of hazmat (links: [(4, 5), (5, 4), (5, 24), (24, 5), (19, 20), (20, 19), (21, 28), (28, 21), (27, 30), (30, 27), (28, 22), (22, 28)]). This means those

links could potentially be opened and still be covered accordingly. Some of those links are uncovered in the MCN solution. This can be observed in Figure 5.5, with the network having a number of available and uncovered links. Moreover, MCN has one link that is used for the transportation of hazmat that is not covered (link (20, 19)), resulting in a CVU of 97.5% (40/41).

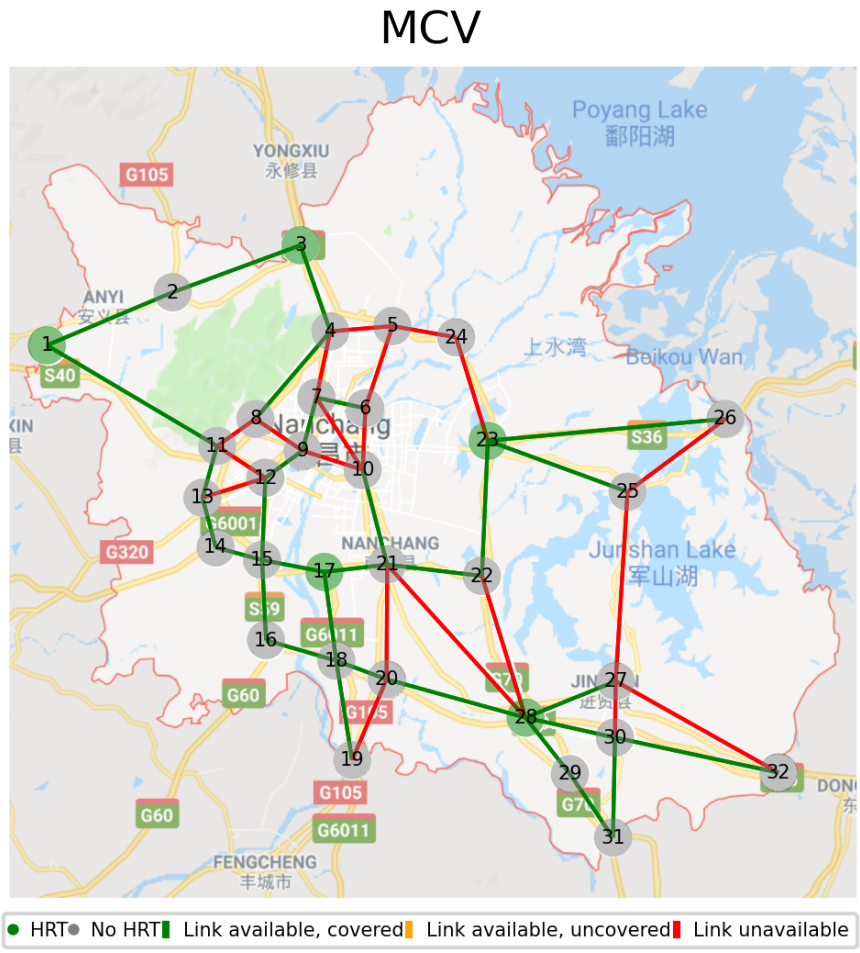

Figure 5.4: MCV: HRT locations and available road links (5 HRTs)

We can also note the differences in locations of the HRTs. As seen in Figure 5.4, MCV positions them at nodes 1,3,17,23, and 30, whereas MCN locates them at nodes 1,3,12,23,

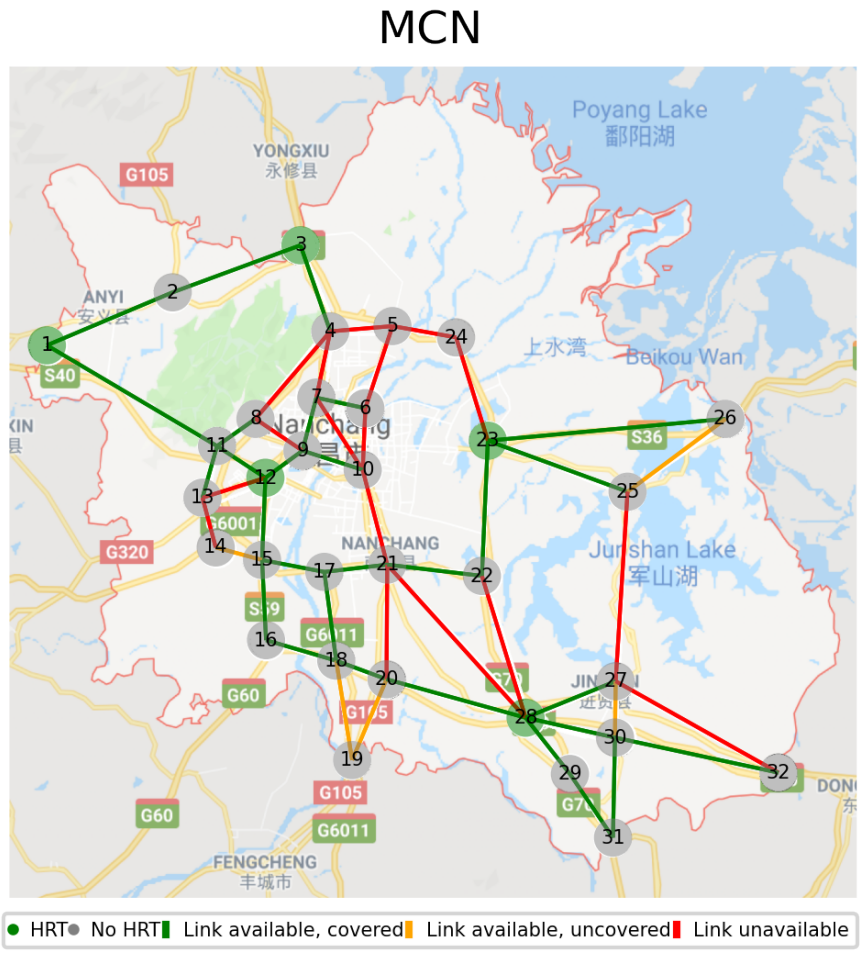

Figure 5.5: MCN: HRT locations and available road links (5 HRTs)

and 28, as shown in Figure 5.5. The difference of two HRT locations, nodes 17 and 30 for MCV and nodes 12 and 28 for MCN, results in better coverage for MCV at the cost of lower connectivity and slightly higher maximum risk, as previously explained.

Additionally, both models generally tend to close links near risky areas. From Figure 5.2, we can observe that the links with higher risks are situated around Nanchang's city center, most notably with links (8,4), (4,5), (9,10), (7,6), (5,6), (6,10), (10,21), and (5,24) having a considerably higher risk compared to other links. We can see in Figures 5.4

and 5.5 that both models close those links, unless going through them is necessary and unavoidable, as Shipments 4, 6, 10 have origins or destinations around those links. This effect can be observed in both Figures 5.6a and 5.6b, where the links with the highest risks are located around the city center close to nodes 12,15,17,21,22.

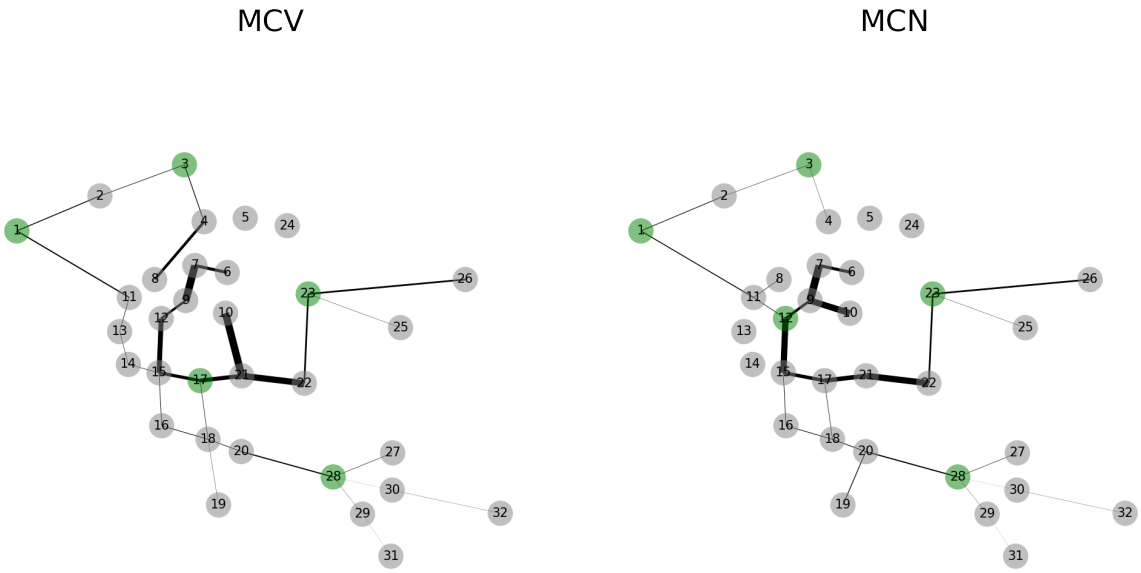

(a) Risk distribution of MCV

(b) Risk distribution of MCN

Figure 5.6: Risk distribution (5 HRTs)

The link availability, the coverage, and HRT location differences become more apparent when looking at a specific shipment. Consider Shipment 4 in Table 5.4 for example. The shipment travels from node 4 to 20, and the resulting paths from models MCV and MCN are respectively shown in Figures 5.7a and 5.7b. We can immediately see that the paths generated by the two models are very different, with MCV having a total distance of 168.8 km and MCN a distance of 71.5 km. The main reason for such a longer route in MCV is that link (8,11) cannot be made available, as it cannot be covered by an HRT nearby. Because of a lack of resources (number of available HRT), MCV cannot place an HRT to cover link (8,11) to lower the risk by providing a shorter route, as all the HRT have to be placed at other nodes to satisfy each of the coverage requirements. This imposes the

closure of that link and forces Shipment 4 to go through links [(8,4), (4,3), (3,2), (2,1), (1,11)]. On the other hand, for MCN, routing through (8,11) is allowed due to the coverage provided by an HRT at node 12, avoiding a long detour and therefore lowering the risk. This, however, comes at the cost of coverage not provided to links [(18,19), (19,18), (19,20), (20,19)], with link (20,18) being used by Shipment 4.

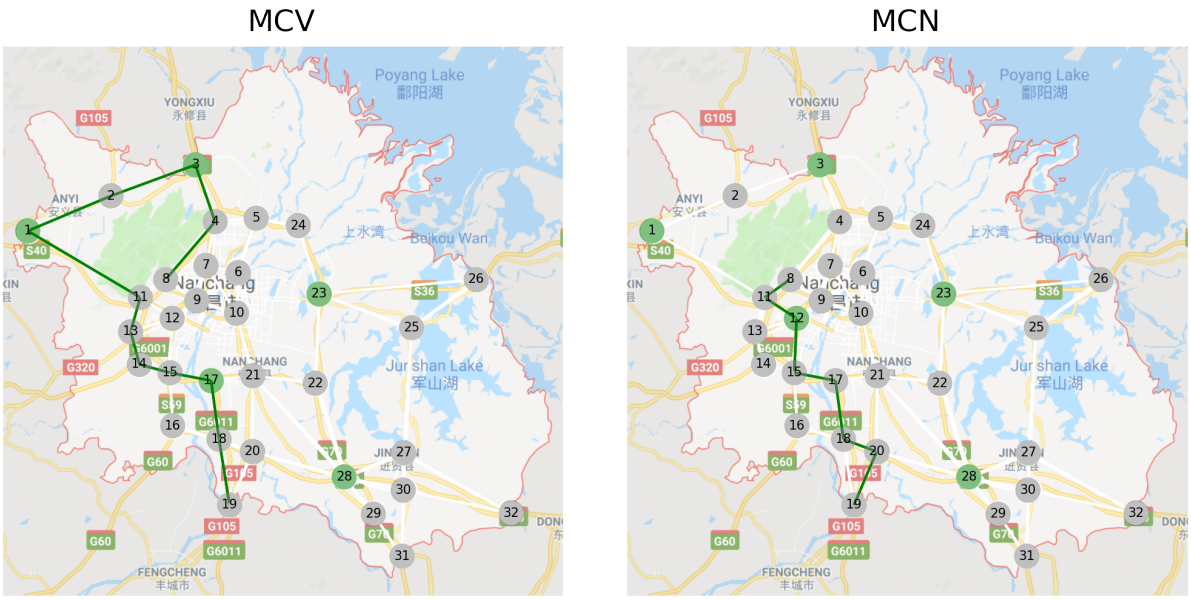

(a) MCV path

(b) MCN path

Figure 5.7: Shipment 4 route comparison (5 HRTs)

When more resources are available, most notably through more HRTs, the solution changes for both models. The total risk and total distance converge to the same values for the two models, as shown in Table 5.7. Unsurprisingly, the risk and distance are lower when compared to the solution with 5 HRTs. Beyond that, for MCN, CN increases from 66.7% to 68.6%, CV goes from 62.7% to 64.7%, and CVU reaches 100%, meaning all the links used are now covered. MCV's values remain the same. Further increasing the number of available HRTs has little effect.

The benefit of the added HRT can be directly seen by looking at the new routes of Shipment 4, respectively shown in Figures 5.8a and 5.8b. Now the path is the same for

Table 5.7: Comparison of Results: MCV & MCN (7 HRTs)

Model	θ	Carriers Distance	CN	CV	CVA	CVU	HRT Locations
MCV	1.48	1,054	60.8%	72.5%	120.4%	100.0%	[1,3,12,17,21,25,28]
MCN	1.48	1,054	68.6%	64.7%	94.1%	100.0%	[2,7,11,16,21,25,28]

both models, taking the shorter route that was not feasible for MCV when only using 5 HRT. Additionally, link (18,19) is now covered by MCN.

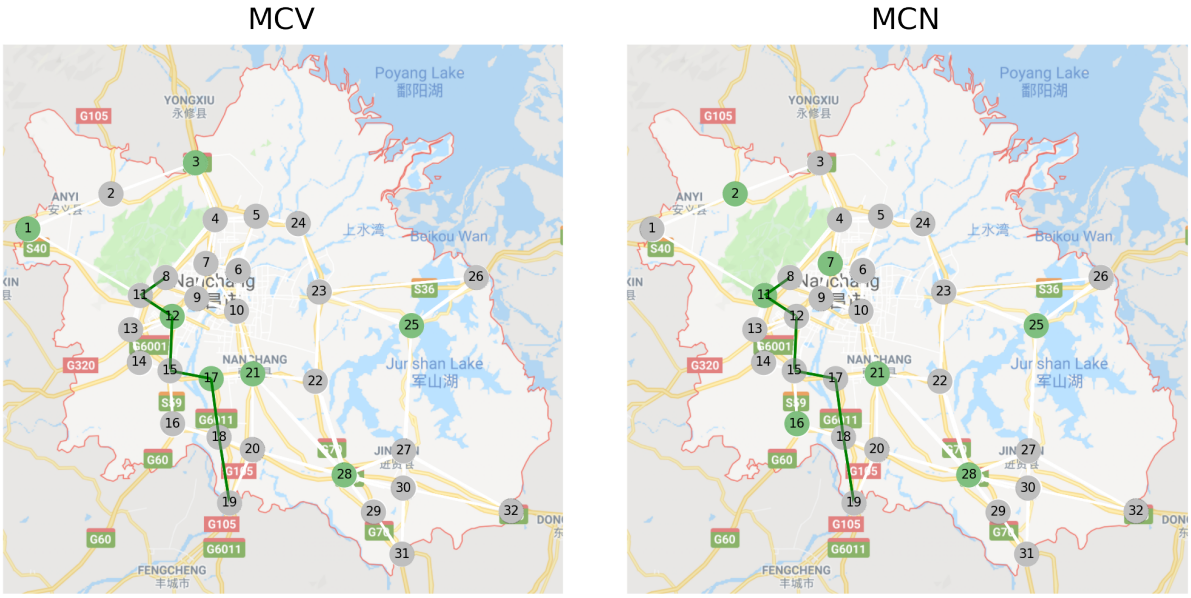

(a) MCV path

(b) MCN path

Figure 5.8: Shipment 4 route comparison (7 HRTs)

In terms of resources, the opposite is also true, as fewer available resources result in worse risk and coverage. We can immediately see from Figure 5.9a that for MCV, 3 HRTs are not sufficient to provide the necessary coverage to all the needed links, resulting in an infeasible problem. MCN is feasible, but with more uncovered links, as shown in Figure 5.9b. The resulting solution of MCN, outlined in Table 5.8, has a higher risk of 1.72 (12.4% increase compared to 5 HRT). Moreover, it leads to worse coverage, having 56.8% of all

links covered, and more importantly, 76.3% of available arcs and 88.1% of the used road segments covered. In addition to that, MCN opens several links around the city center, which it would otherwise avoid. It is interesting to note, however, that the connectivity of MCN increases in this case. That is likely because MCN leverages shorter routes (lower total carriers' distance) to reduce risk given, the limited possible coverage, and opens more links as a result.

Table 5.8: Comparison of Results: MCV & MCN (3 HRTs)

Model	θ	Carriers' Distance	CN	CV	CVA	CVU	HRT Locations
MCV	-	-	-	-	-	-	-
MCN	1.72	975	74.5%	56.8%	76.3%	88.1%	[9,20,23]

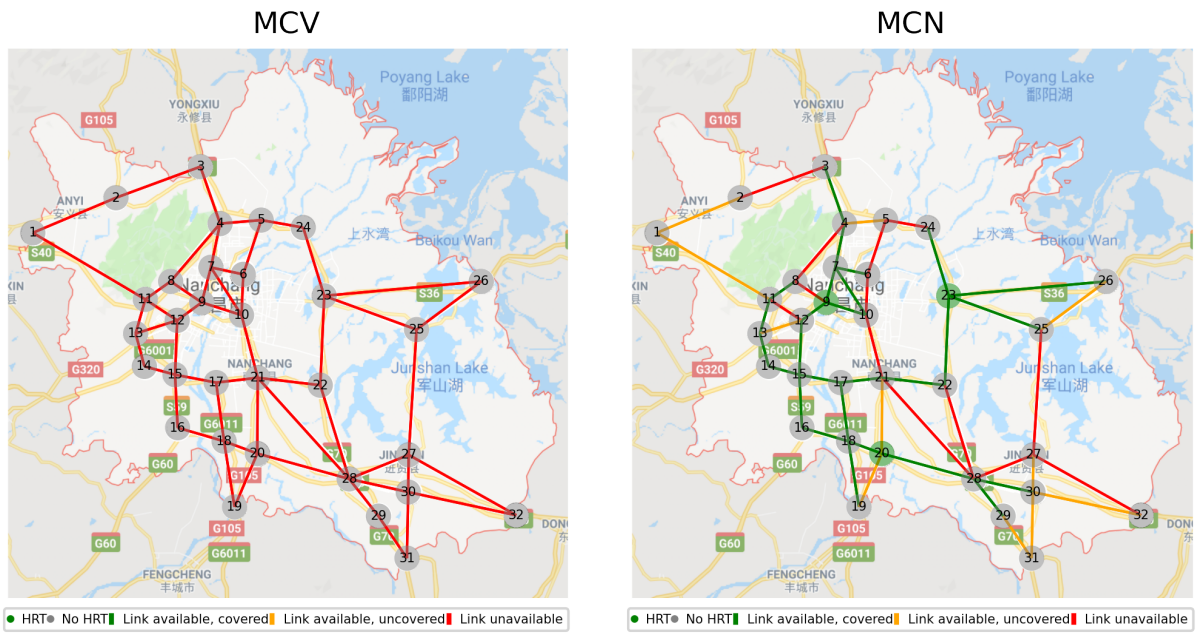

(a) MCV path

(b) MCN path

Figure 5.9: HRT locations and available road links (3 HRTs)

Finally, we examine the effect of an increased number of shipments on the solution (5 HRT). The results are summarized in Table 5.9. We can see that the connectivity of the

network (CN) increases for both models, going from 60.8% to 66.7% for MCV and 66.7% to 68.7% for MCN. This can be explained by the fact that the shipments' origins and destinations are more spatially spread throughout the network, forcing the model to open more links as result. Moreover, MCN's coverage also increases, as CV goes from 62.7% to 68.6% and all the links that are available and used, are now covered.

Table 5.9: Comparison of Results: MCV & MCN (30 shipments, 5 HRTs)

Model	θ	Carriers Distance	CN	CV	CVA	CVU	HRT Locations
MCV	6.01	2,495	66.7%	72.5%	108.2%	100.0%	[1,7,17,23,28]
MCN	5.94	2,541	68.6%	68.6%	100.0%	100.0%	[1,7,17,23,28]

The example of Shipment 4 highlights the key difference between the two formulations. MCV guarantees the coverage of the opened links leading to high system coverage (CV), but doing so might lead to increased total system cost and lower connectivity (CN). On the other hand, MCN allows a more relaxed solution with higher connectivity and prioritizes lower total risk at the cost of leaving some arcs to be uncovered. That results in lower coverage, and could therefore be prone to potential accidents being left unattended for a much longer time period, which may lead to undesirable outcomes for the surrounding residents.

The disadvantage of MCV is that the problem may be infeasible, or may result in a disconnected network, for some shipment sets, if the available emergency resources (number of HRTs) are insufficient. However, within the context of a pessimistic formulation, MCV is a better model, as it can properly control the risk at all potential accident locations. Moreover, MCV is more sensitive to available resources. Sufficient resources can largely reduce the system risk by ensuring the coverage, while at the same time maintaining specifiable connectivity. Nevertheless, MCN appears to be more sensitive to changes in number of shipments, which force a better overall coverage. In this sense, MCV can ensure a more robust transportation system when the shipment details are highly uncertain.

5.4 Comparison of Risk Pessimism and Risk Equity

Pessimism is a critical aspect of the model we propose, as it emphasizes the desire to account for the maximum risk on the network from the government agency's perspective. In the meantime, "risk equity", reflecting the fair spatial distribution of risk, has drawn much public attention lately, especially to those who live around the regions loaded with hazmats. In this section, we compare our pessimistic risk objective to risk equity through a trade-off analysis.

In particular, the min max method is employed here to find the safest set of paths. We define μ to be the maximum link risk, and then substitute Eqns. (4.3) and (4.4) by the following expressions to minimize the maximum link risk.

$$\min \quad \mu \tag{5.6}$$

$$\text{s.t.} \quad \sum_{m\in\mathcal{N}}\sum_{c\in\mathcal{C}} R_{ij}^{c}\alpha(t_{ij}^{m})h_{ij}^{mc} \leq \mu \qquad \forall (i,j)\in\mathcal{A} \tag{5.7}$$

Figure 5.10 compares the total risk for 10, 30, and 50 random shipment sets (20 instances each). We can clearly see that minimizing the maximum link risk results in increased network risk. Besides, larger shipment sets lead to broader ranges of risk equity.

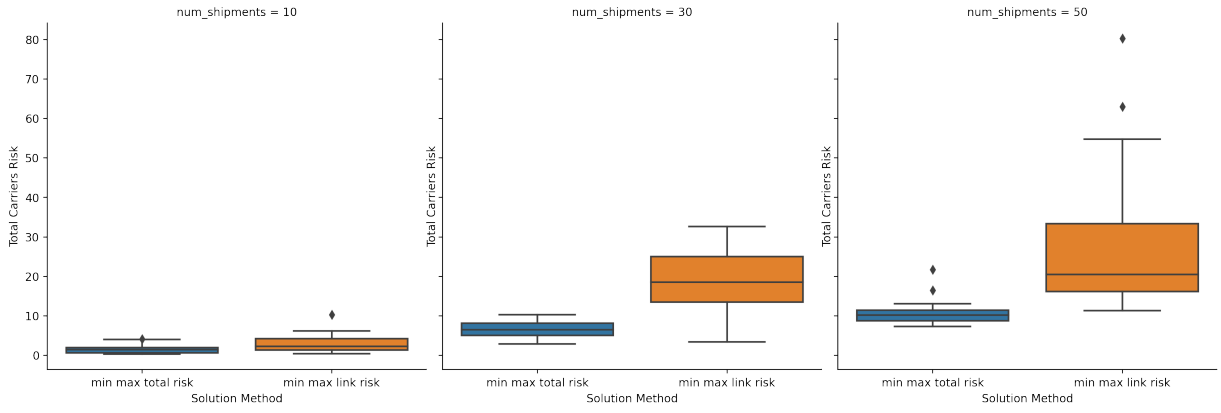

Figure 5.10: Comparison of Approaches

Additionally, to better understand the trade-off between pessimism and risk equity, we perform a trade-off analysis between the two approaches. We adopt a weighting factor

$0 \leq w \leq 1$ to balance the maximum total risk on the network, θ, as per our normal model, and the maximum link risk, μ. The following expressions replace Eqns. (4.3) and (4.4), while the remainder of the model stays the same.

$$\min \quad w\theta + (1-w)\mu \tag{5.8}$$

$$\text{s.t.} \quad \sum_{m\in\mathcal{N}} \sum_{(i,j)\in\mathcal{A}} \sum_{c\in\mathcal{C}} R_{ij}^{c}\alpha(t_{ij}^{m})h_{ij}^{mc} \leq \theta \tag{5.9}$$

$$\sum_{m\in\mathcal{N}} \sum_{c\in\mathcal{C}} R_{ij}^{c}\alpha(t_{ij}^{m})h_{ij}^{mc} \leq \mu \qquad \forall (i,j) \in \mathcal{A} \tag{5.10}$$

Objective (5.8) assesses the weighted sum of θ and μ. Eqn. (5.9) represents the maximum risk on the network, and Eqn. (5.10) is the maximum risk on a link.

We compare the solutions obtained by using both methods, in terms of MCV and MCN, with shipment set given in Table 5.4. The results are summarized in Tables 5.10 and 5.11, contrasting the maximum link risk (μ) and maximum total network risk (θ) from MCV and MCN respectively. There exists a clear trade-off between risk equity and system risk, as shown in Figure 5.11a for MCV, and Figure 5.11b for MCN, as an increased θ results in a lower μ, and vice-versa. There is not much difference between the MCV and MCN trade-off curves; both exhibit the same behavior. We notice a slightly lower optimal μ for MCN compared to MCV (0.215 vs 0.216). Moreover, the system risk caused by optimal μ is greater for MCV than for MCN (3.61 vs 2.87).

Table 5.10: Trade-off: MCV

θ	μ	HRT Locations
3.61	0.216	[3, 6, 17, 23, 28]
1.68	0.216	[1, 5, 17, 23, 28]
1.62	0.219	[1, 5, 17, 23, 28]
1.60	0.222	[1, 3, 17, 28, 30]

Table 5.11: Trade-off: MCN

θ	μ	HRT Locations
2.87	0.215	[5, 10, 12, 13, 21]
1.58	0.215	[1, 3, 17, 23, 28]
1.55	0.216	[1, 3, 17, 23, 28]
1.53	0.222	[1, 3, 17, 23, 28]

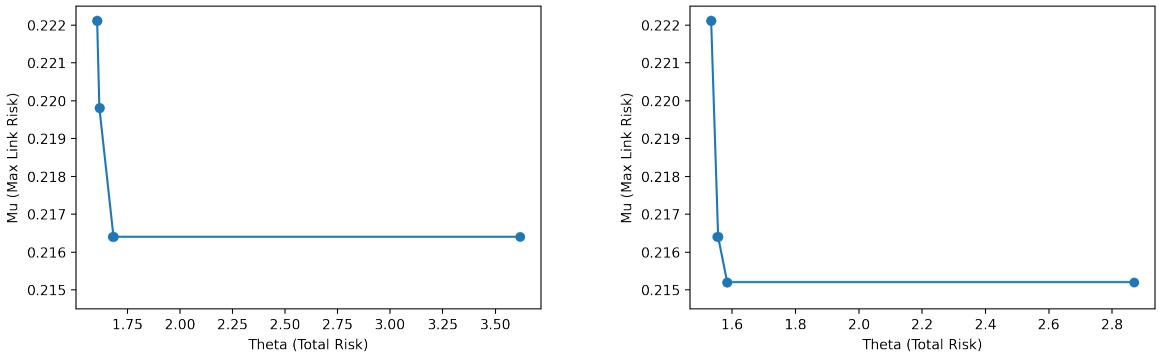

(a) MCV (b) MCN

Figure 5.11: Trade-off between θ and μ

5.5 Comparison of Risk Mitigation Mechanisms

The present study integrates two mechanisms, namely the network design and emergency response, to mitigate the network risk associated with hazmat transportation. To explore the benefits of these risk mitigation mechanisms, we solve the problems under the following individual settings. Comparison of results with MCV and MCN are listed in Table 5.12.

No risk mitigation (NRM) All network links are available for hazmat shipments. This setting essentially corresponds to minimizing the total carriers' distance and calculating the risk that the shipments pose. This is obtained by setting all the links to be available ($y_{ij} = 1$) and $H = 0$ in the MCN model. NRM shows the maximum risk the shipment set poses without any mitigation mechanism.

Hazmat Transportation Network Design (HTND) A network is designed to minimize the maximum risk by deciding which links to open and close to hazmat shipments. This can be formulated by setting $H = 0$ in MCN. HTND emphasizes the network design aspect, and its efficacy in reducing risk.

HRT Only (HRTO) All links are available and the locations for HRT are optimized to minimize the maximum network risk. This setting is equivalent to minimizing

the distance, and maximizing the emergency coverage by forcing all the links to be available ($y_{ij} = 1$) in MCN. HRTO outlines the effectiveness that coverage of used links has on reducing risk.

Table 5.12: Risk Mitigation Mechanisms Comparison

Model	θ	Carriers Distance	CN	CV	CVA	CVU	HRT Locations
NRM	34.84	784	100%	0%	0%	0%	-
HTND	7.42	1,127	64.7%	0%	0%	0%	-
HRTO	6.98	784.1	100%	60.7%	60.7%	97.5%	[6, 7, 17, 23, 28]
MCV	1.61	1,144	60.8%	72.5%	120.4%	100.%	[1, 3, 17, 23, 30]
MCN	1.53	1,077	66.7%	62.7%	94.1%	97.5%	[1, 3, 12, 23, 28]

It can be observed from Table 5.12 that NRM performs the worst in terms of risk. Risk is not mitigated in any way, with a value here of more than 20 times greater than for MCV or MCN. From there, single risk mitigation technique models greatly reduce the risk on their own, with HTND and HRTO having a risks of 7.42 and 6.48 respectively, resulting in a $\sim$80% risk reduction. While the risk mitigation provided by both HTND and HRTO alone is considerable, the combination of network design and emergency coverage provides the best possible combination of factors to reduce risk, with MCV and MCN resulting in lower risk. As expected, NRM and HRTO have 100% connectivity and result in the same total distance, while NRM and HTND have 0% coverage.

Figures 5.12a and 5.12b further illustrate the available links and HRT locations respectively under the HTND and HRTO settings. (The NRM setting has no restrictions on links and considers no HRT, and therefore is not included here.) Also note that the sequential combination of HTND and HRTO is very similar to the heuristic solution algorithm proposed in Chapter 4.

From the resulting networks, we can see in Figure 5.12a that HTND avoids city center links unless necessary, similarly to MCV and MCN, as HTND has the sufficient connectivity to shape the network to go around it. Moreover, from Figure 5.12b, we can observe that HRTO locates two HRTs in the city center, as those links result in shorter routes, to mitigate the resulting high risk.

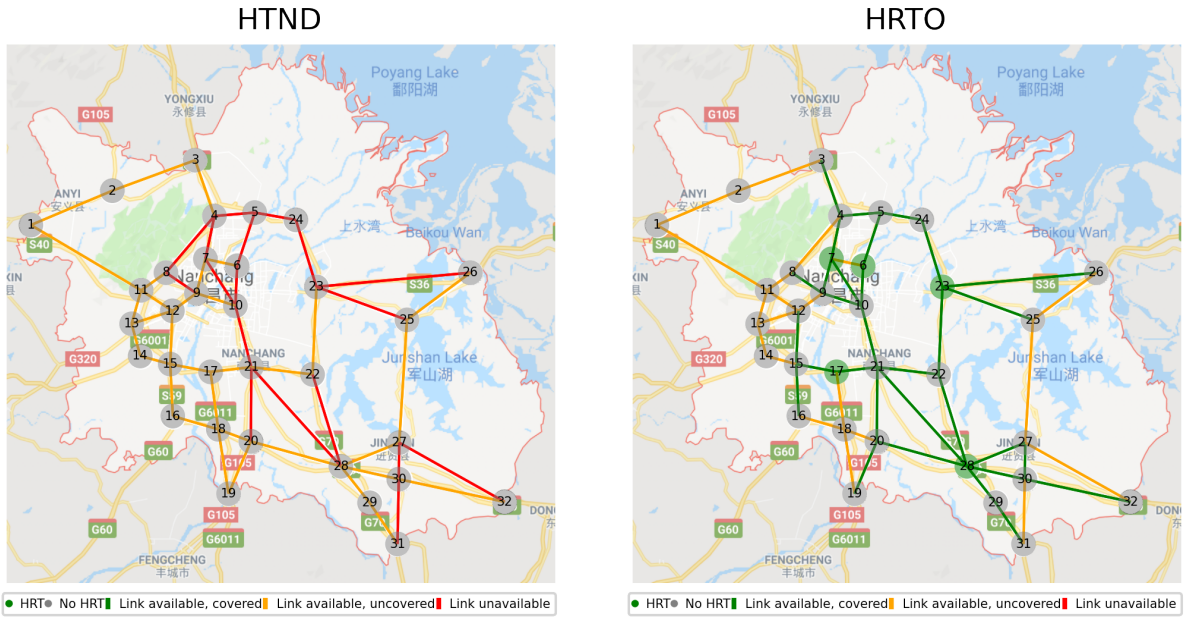

(a) HTND

(b) HRTO

Figure 5.12: HRT locations and available road links for HTND and HRTO

5.6 Sensitivity Analyses

Finally, we perform a series of sensitivity analyses around several key parameters of our model. This allows us to examine how changing those parameters affects the optimal solution, i.e. the total risk on the network, and to better understand the behavior of our model under different settings. We propose three categories to represent the low, medium, and high factors, and propose a value for each parameter. These are summarized in Table 5.13. The medium category indicates the base case given in Table 5.3.

5.6.1 T_{best}, T_{worst}

We increase and decrease T_{best} and T_{worst} respectively by 5 and 10 minutes to observe how changes in desired coverage times affect the solutions of MCV and MCN. The results are

Table 5.13: Sensitivity Analysis - Summary of Parameters

Parameter	Notation	Value		
		Low	Mid	High
Best and worst response times	T_{best}, T_{worst} (min)	20, 40	25, 50	30, 60
Service satisfaction rates	γ, β	70%, 80%	80%, 90%	90%, 95%
Variance of response time	η as in $(\sigma_{ij}^m)^2 = \eta t_{ij}^m$	0.05	0.25	0.5
RTF percentile	ω as in $\alpha(t_{ij}^{m\omega})$[1]	10th	50th	90th

[1] $\alpha(\cdot)$ represents the function used to compute the RTF and $t_{ij}^{m\omega}$ being the ω-th percentile value of the Normal distribution T_{ij}^m.

presented in Table 5.14.

Table 5.14: Sensitivity Analysis: Response Time

T_{best}, T_{worst}	Model	θ	Total Distance	CN	CV	CVA	CVU	HRT Locations
20/40	MCV	-	-	-	-	-	-	-
	MCN	1.53	1,027	70.6%	50.9%	72.2%	84.6%	[4, 15, 22, 25, 28]
25/50	MCV	1.61	1,144	60.8%	72.5%	120.4%	100.0%	[1, 3, 17, 23, 30]
	MCN	1.53	1,077	66.7%	62.7%	94.1%	97.5%	[1, 3, 12, 23, 28]
30/60	MCV	1.48	1,127	64.7%	76.5%	118.2%	100.0%	[2, 11, 12, 28, 25]
	MCN	1.48	1,127	74.5%	70.5%	94.7%	100.0%	[2, 11, 15, 25, 28]

By decreasing the required coverage time, we impose faster response times to accidents. MCV is infeasible under this condition, i.e., a solution that would satisfy the desired coverage times for the given resources (H=5) is not available. This result further illustrates the fact that MCV requires enough resources to be applicable. MCN, whilst being feasible, has a lower coverage as a result, as the shorter desired time forces the response time to some links to be too long to allow coverage. CV drops to 50.9% and 72.2% of all available links, and 86.4% of all used links are now covered.

On the other hand, increasing the desired response time has the opposite effect. The solutions of MCV and MCN converge to the same solution with lower risk, similarly to increasing the number of HRT, as previously explained. The degrees of coverage of both

models increase as a result, most notably with MCN now covering all the links used. Interestingly, increasing the desired coverage times beyond 30 and 60 for T_{best} and T_{worst} respectively does not further reduce risk. Starting from 30/60, all the links used are covered according to the lowest RTF value (see Table 5.2). This shows a trade-off between desired coverage times and coverage level. Relaxing the coverage time by allowing longer response times inevitably leads to better coverage.

5.6.2 Emergency Service Satisfaction Rates (β, γ)

We now vary γ and β, the optimistic and pessimistic coverage time probabilities, which indicate the satisfaction rates of emergency services. The results are given in Table 5.15.

Table 5.15: Sensitivity Analysis: γ, β

γ, β	Model	θ	Total Distance	CN	CV	CVA	CVU	HRT Locations
0.7, 0.8	MCV	1.50	1,049	60.7%	72.5%	119.4%	100.0%	[1, 3, 17, 23, 28]
	MCN	1.50	1,049	72.5%	58.8%	81.1%	100.0%	[1, 3, 17, 23, 28]
0.8, 0.9	MCV	1.61	1,144	60.8%	72.5%	120.4%	100.0%	[1, 3, 17, 23, 30]
	MCN	1.53	1,077	66.7%	62.7%	94.1%	97.5%	[1, 3, 12, 23, 28]
0.9, 0.95	MCV	1.62	968	60.7%	70.5%	116.1%	100.0%	[1, 9, 18, 23, 30]
	MCN	1.54	1,008	60.7%	52.9%	87.1%	97.5%	[1, 9, 20, 23, 30]

Decreasing γ, β means that the coverage constraints are more easily satisfied, as the probabilities of $P(T_{ij}^m h_{ij}^m \leq T_{best})$ and $P(T_{ij}^m h_{ij}^m \leq T_{worst})$ can be lower and still meet the coverage constraints; while increasing γ, β has the opposite effect. This phenomenon is applicable for both MCV and MCN, and can clearly be seen in Table 5.15, as the risk decreases with lower probabilities. We can also observe that the MCV risk reduces by a greater factor than MCN, indicating that MCV is more sensitive to changes in γ, β.

As a result of decreasing γ, β, MCN covers all the links that are used. However, this cannot be extended to the other connectivity factors CV and CVA. However, this could also be due to the fact that increasing those values has no effect on the risk measured. Moreover, MCN's connectivity appears to increase with lower γ, β, but the same cannot be said for MCV.

5.6.3 Variance of Response Time (η)

Next, we change the response time variance, whose results are summarized in Table 5.16.

Table 5.16: Sensitivity Analysis: Response Time Variance

η	Model	θ	Total Distance	CN	CV	CVA	CVU	HRT Locations
0.05	MCV	1.50	1,049	62.7%	68.3%	109.4%	100.0%	[1, 3, 17, 23, 28]
	MCN	1.50	1,049	58.8%	58.8%	100.0%	100.0%	[1, 3, 17, 23, 28]
0.25	MCV	1.61	1,144	60.8%	72.5%	120.4%	100.0%	[1, 3, 17, 23, 30]
	MCN	1.53	1,077	66.7%	62.7%	94.1%	97.5%	[1, 3, 12, 23, 28]
0.50	MCV	1.62	968	60.7%	70.5%	116.1%	100.0%	[1, 9, 18, 23, 30]
	MCN	1.54	1,008	60.7%	52.9%	87.1%	97.5%	[1, 9, 20, 23, 30]

The variance of the normal distribution indicates the "width" of the distribution, and determines the probability that the desired coverage time can be met. Because of this relationship between the variance and γ and β, the same observations made for the coverage time probabilities are applicable to the variance of response time. In fact, the resulting risk and distance changes are identical. We can see that decreasing the variance leads to lower system risk.

Additionally, for MCN, the coverage of available links and of the road segments used rises with lower variance. MCN reaches 100% coverage of available links and 100% coverage of used links.

5.6.4 Response Time Factor (RTF) Percentile

Finally, we analyze the effect of varying the percentile of the RTF for risk computation. We define $t_{ij}^{m\omega}$ to be the argument of the α function, with ω indicating the percentile value of the Normal distribution T_{ij}^{m}, and use the 10th, 50th and 90th percentiles. Note that our basic model applies the 50th percentile, i.e., the mean value. Also, $\eta = 0.5$ is used, as a "wider" distribution that enhances the effect of the chosen percentile. The results are summarized in Table 5.17.

Lowering ω does not seem to affect the solution, as the risks of both MCV and MCN are identical to the base case (1.61 and 1.54, respectively), and the connectivity and coverage

Table 5.17: Sensitivity Analysis: Response Time Factor (RTF) Percentile

ω (percentile)	Model	θ	Total Distance	CN	CV	CVA	CVU	HRT Locations
10th	MCV	1.62	968	60.7%	70.5%	116.1%	100.0%	[1, 9, 18, 23, 30]
	MCN	1.54	1,008	60.7%	52.9%	87.1%	97.5%	[1, 9, 20, 23, 30]
50th	MCV	1.62	968	60.7%	70.5%	116.1%	100.0%	[1, 9, 18, 23, 30]
	MCN	1.54	1,008	60.7%	52.9%	87.1%	97.5%	[1, 9, 20, 23, 30]
90th	MCV	1.71	1,143	56.8%	70.5%	124.1%	100.0%	[1, 3, 17, 23, 30]
	MCN	1.61	974	68.6%	58.8%	85.7%	95%	[1, 9, 17, 23, 28]

are also the same. On the other hand, increasing ω results in a worse solution, since it increases the response time, and therefore leads to a higher risk. Specifically looking at the discrete RTF function implemented in this case study (detailed in Table 5.2), raising the response time results in higher RTF due to the comparison with T_{best}. As a result, θ increases to 1.71 and 1.61 for MCV and MCN respectively. The connectivity of MCV reduces from 60.7% to 56.8%, while the opposite is true for MCN, as the connectivity grows from 60.7% to 68.8%. Finally, the coverage of MCV is not affected, while MCN's coverage increases in terms of CV, but, more importantly, decreases in terms of CVA (from 87.1% of available and covered links to 85.7%) and CVU (from 97.5% of links used and covered to 95%), thus resulting in a worse solution.

Chapter 6

Conclusion and Future Research

This thesis studies a pessimistic hazmat network design problem with emergency team location considering uncertain response time. More specifically, in a bilevel model, the upper-level represents the network design decision of the authority (government), aiming to minimize the risk through the availability of network segments and location of hazmat response teams. The lower-level reflects the hazmat carriers' routing decisions to minimize the transportation costs. Two variants of pessimistic formulations with chance constraints are developed and compared in terms of connectivity and coverage. The optimal solution can be obtained through a reformulation of the original model into a single-level format for smaller problems, whereas for large instances, a heuristic is outlined and shown to yield good approximate solutions in a computationally efficient manner.

The models and algorithms are then applied to a real-world highway hazmat transportation network for additional analyses. The practical implications revealed by our numerical experiments are summarized as follows.

1. It is shown that the pessimistic assumption can better control the follower's non-cooperative behavior in choosing the best shipping paths, and well-located HRTs can further reduce the risk associated with hazmat transportation. Moreover, emergency service satisfaction can be ensured by posing best and worst response times, and embedding the corresponding coverage probabilities into the government's decision.

2. Through the comparison of the two formulations, we can see that MCV (Model Coverage) secures the coverage of all hazmat shipments and is more robust to shipment uncertainties, while MCN (Model Connectivity) provides more flexible solutions to limited emergency resources. Based on this observation, it is suggested that MCN can be implemented as a first step when the resources are restricted. As resources become sufficient, the MCV solution can be employed to guarantee the coverage of the entire network. More resources lead to both higher coverage and higher emergency service satisfaction.

3. The two proposed mechanisms, namely network design and emergency coverage, can be used individually or jointly to significantly reduce network risk. Especially when they are applied together, the network risk can be mitigated by more than 95% compared to the situation with no risk mitigation mechanism. Even with only one mechanism, the improvement rate can achieve approximately 80%.

4. Improving the efficiency of emergency service can also be achieved by upgrading the road network (such that the incident rate can be reduced, and HRTs can navigate faster), building alternative paths for HRTs (to avoid possible congestion caused by the incidents), and employing mobile HRTs patrolling over rural areas (especially when those areas cannot be covered by HRTs at fixed locations).

Several additional directions can be explored in the future.

1. The pessimistic model can be applied to other hazmat-related problems, such as determining the optimal dual toll policy for a hazmat transportation network. Incorporating both network design and toll setting to mitigate the hazmat transportation risk would also be an interesting direction.

2. Real-world situations are full of unexpected changes and variations. So, the uncertainty and disruption issues should be integrated into designing a well-connected and well-covered hazmat network.

3. The model proposed could be further enhanced by making it more realistic, although that may not be practical. These features may include the coverage of a link by

multiple emergency response teams, the inclusion of other types of traffic, and the interaction of multiple hazmat shipments on a link and the resulting risks.

4. It would also be extremely interesting, yet challenging, to examine the time-dependent hazmat network design problem.

References

Abkowitz, M. and Cheng, P. D.-M. (1988), 'Developing a risk/cost framework for routing truck movements of hazardous materials', *Accident Analysis & Prevention* **20**(1), 39–51.

Abkowitz, M., Lepofsky, M. and Cheng, P. (1992), 'Selecting criteria for designating hazardous materials highway routes', *Transportation Research Record* **1333**(2.2).

US FMCSA (2019), 'How to comply with federal hazardous materials regulations'. **URL:** *https://www.fmcsa.dot.gov/regulations/hazardous-materials/how-comply-federal-hazardous-materials-regulations*

US PHMSA (2021), 'Phmsa's hazardous materials incident statistic reports 2011-2020'. **URL:** *https://www.phmsa.dot.gov/hazmat-program-management-data-and-statistics/data-operations/incident-statistics*

Aiyoshi, E. and Shimizu, K. (1981), 'Hierarchical decentralized systems and its new solution by a barrier method.', *IEEE Transactions on Systems, Man and Cybernetics* (6), 444–449.

Amaldi, E., Bruglieri, M. and Fortz, B. (2011), On the hazmat transport network design problem, *in* 'International Conference on Network Optimization', Springer, pp. 327–338.

Ban, X. J., Lu, S., Ferris, M. and Liu, H. X. (2009), Risk averse second best toll pricing, *in* 'Transportation and Traffic Theory 2009: Golden Jubilee', Springer, pp. 197–218.

Bard, J. F. (1991), 'Some properties of the bilevel programming problem', *Journal of optimization theory and applications* **68**(2), 371–378.

Bard, J. F. and Falk, J. E. (1982), 'An explicit solution to the multi-level programming problem', *Computers & Operations Research* **9**(1), 77–100.

Batta, R. and Chiu, S. S. (1988), 'Optimal obnoxious paths on a network: Transportation of hazardous materials', *Operations research* **36**(1), 84–92.

Berman, O., Verter, V. and Kara, B. Y. (2007), 'Designing emergency response networks for hazardous materials transportation', *Computers & operations research* **34**(5), 1374–1388.

Bracken, J. and McGill, J. T. (1973), 'Mathematical programs with optimization problems in the constraints', *Operations Research* **21**(1), 37–44.

Cao, D. and Leung, L. C. (2002), 'A partial cooperation model for non-unique linear two-level decision problems', *European Journal of Operational Research* **140**(1), 134–141.

Church, R. L. and Meadows, M. E. (1979), 'Location modeling utilizing maximum service distance criteria', *Geographical Analysis* **11**(4), 358–373.

Church, R. and ReVelle, C. (1974), The maximal covering location problem, *in* 'Papers of the regional science association', Vol. 32, Springer-Verlag, pp. 101–118.

Dempe, S. (2020), Bilevel optimization: Theory, algorithms, applications and a bibliography, *in* 'Bilevel Optimization', Springer, pp. 581–672.

Dempe, S., Mordukhovich, B. S. and Zemkoho, A. B. (2014), 'Necessary optimality conditions in pessimistic bilevel programming', *Optimization* **63**(4), 505–533.

Erkut, E. and Alp, O. (2007), 'Designing a road network for hazardous materials shipments', *Computers & Operations Research* **34**(5), 1389–1405.

Erkut, E. and Gzara, F. (2008), 'Solving the hazmat transport network design problem', *Computers & Operations Research* **35**(7), 2234–2247.

Erkut, E. and Ingolfsson, A. (2000), 'Catastrophe avoidance models for hazardous materials route planning', *Transportation Science* **34**(2), 165–179.

Erkut, E., Tjandra, S. A. and Verter, V. (2007), 'Hazardous materials transportation', *Handbooks in operations research and management science* **14**, 539–621.

Erkut, E. and Verter, V. (1998), 'Modeling of transport risk for hazardous materials', *Operations research* **46**(5), 625–642.

Federal Motor Carrier Safety Administration (2018), 'Large truck and bus crash facts 2016'.
URL: *https://www.fmcsa.dot.gov/sites/fmcsa.dot.../ltbcf-2016-final-508c-may-2018.pdf*

Fontaine, P. and Minner, S. (2018), 'Benders decomposition for the hazmat transport network design problem', *European Journal of Operational Research* **267**(3), 996–1002.

Guo, X. and Liu, H. X. (2011), 'Bounded rationality and irreversible network change', *Transportation Research Part B: Methodological* **45**(10), 1606–1618.

Gzara, F. (2013), 'A cutting plane approach for bilevel hazardous material transport network design', *Operations Research Letters* **41**(1), 40–46.

Hamouda, G., Saccomanno, F. and Fu, L. (2004), 'Quantitative risk assessment decision-support model for locating hazardous materials teams', *Transportation research record* **1873**(1), 1–8.

Hosseini, S. D. and Verma, M. (2018), 'Conditional value-at-risk (cvar) methodology to optimal train configuration and routing of rail hazmat shipments', *Transportation Research Part B: Methodological* **110**, 79–103.

Jeroslow, R. G. (1985), 'The polynomial hierarchy and a simple model for competitive analysis', *Mathematical programming* **32**(2), 146–164.

Jiahong, Z. and Bin, S. (2010), A new multi-objective model of location-allocation in emergency response network design for hazardous materials transportation, *in* '2010 IEEE International Conference on Emergency Management and Management Sciences', IEEE, pp. 246–249.

Jorion, P. et al. (2007), *Financial risk manager handbook*, Vol. 406, John Wiley & Sons.

Kang, Y., Batta, R. and Kwon, C. (2014*a*), 'Generalized route planning model for hazardous material transportation with var and equity considerations', *Computers & Operations Research* **43**, 237–247.

Kang, Y., Batta, R. and Kwon, C. (2014*b*), 'Value-at-risk model for hazardous material transportation', *Annals of Operations Research* **222**(1), 361–387.

Kara, B. Y. and Verter, V. (2004), 'Designing a road network for hazardous materials transportation', *Transportation Science* **38**(2), 188–196.

Ke, G. Y., Zhang, H. and Bookbinder, J. H. (2020), 'A dual toll policy for maintaining risk equity in hazardous materials transportation with fuzzy incident rate', *International Journal of Production Economics* **227**, 107650.

Kolstad, C. D. and Lasdon, L. S. (1990), 'Derivative evaluation and computational experience with large bilevel mathematical programs', *Journal of optimization theory and applications* **65**(3), 485–499.

Küçükyavuz, S. and Jiang, R. (2021), 'Chance-constrained optimization: A review of mixed-integer conic formulations and applications', *arXiv preprint arXiv:2101.08746* .

Kwon, C. (2011), Conditional value-at-risk model for hazardous materials transportation, *in* 'Proceedings of the 2011 winter simulation conference (WSC)', IEEE, pp. 1703–1709.

Li, R., Chai, H. and Tang, J. (2013), 'Empirical study of travel time estimation and reliability', *Mathematical Problems in Engineering* **2013**.

List, G. F. (1993), Siting emergency response teams: tradeoffs among response time, risk, risk equity and cost, *in* 'Transportation of hazardous materials', Springer, pp. 117–133.

List, G. F. and Turnquist, M. A. (1998), 'Routing and emergency-response-team siting for high-level radioactive waste shipments', *IEEE Transactions on Engineering Management* **45**(2), 141–152.

Liu, J., Fan, Y., Chen, Z. and Zheng, Y. (2018), 'Pessimistic bilevel optimization: a survey', *International Journal of Computational Intelligence Systems* **11**(1), 725–736.

Lozano, L. and Smith, J. C. (2017), 'A value-function-based exact approach for the bilevel mixed-integer programming problem', *Operations Research* **65**(3), 768–786.

Marcotte, P., Mercier, A., Savard, G. and Verter, V. (2009), 'Toll policies for mitigating hazardous materials transport risk', *Transportation science* **43**(2), 228–243.

Marcotte, P., Savard, G. and Zhu, D. (2001), 'A trust region algorithm for nonlinear bilevel programming', *Operations research letters* **29**(4), 171–179.

Marianov, V. and Serra, D. (1998), 'Probabilistic, maximal covering location—allocation models for congested systems', *Journal of Regional Science* **38**(3), 401–424.

Patel, M. H. and Horowitz, A. J. (1994), 'Optimal routing of hazardous materials considering risk of spill', *Transportation Research Part A: Policy and Practice* **28**(2), 119–132.

ReVelle, C., Cohon, J. and Shobrys, D. (1991), 'Simultaneous siting and routing in the disposal of hazardous wastes', *Transportation Science* **25**(2), 138–145.

ReVelle, C., Toregas, C. and Falkson, L. (1976), 'Applications of the location set-covering problem', *Geographical analysis* **8**(1), 65–76.

Saccomanno, F. and Allen, B. (1987), 'Locating emergency response capability for dangerous goods incidents on a road network', *Transportation of Hazardous Materials* **1**.

Saccomanno, F. F. and Chan, A.-W. (1985), *Economic evaluation of routing strategies for hazardous road shipments*, number 1020.

Simon, H. A. (1956), 'Rational choice and the structure of the environment.', *Psychological review* **63**(2), 129.

Sinha, A., Malo, P. and Deb, K. (2017), 'A review on bilevel optimization: from classical to evolutionary approaches and applications', *IEEE Transactions on Evolutionary Computation* **22**(2), 276–295.

Sivakumar, R. A. and Batta, R. (1994), 'The variance-constrained shortest path problem', *Transportation Science* **28**(4), 309–316.

Sivakumar, R. A., Batta, R. and Karwan, M. H. (1993), 'A network-based model for transporting extremely hazardous materials', *Operations Research Letters* **13**(2), 85–93.

Stackelberg, H. v. et al. (1952), 'Theory of the market economy'.

Takalloo, M. and Kwon, C. (2020), 'On the price of satisficing in network user equilibria', *Transportation Science* **54**(6), 1555–1570.

Taslimi, M., Batta, R. and Kwon, C. (2017), 'A comprehensive modeling framework for hazmat network design, hazmat response team location, and equity of risk', *Computers & Operations Research* **79**, 119–130.

Transportation Research Board and National Academies of Sciences, Engineering, and Medicine (2011), *A Guide for Assessing Community Emergency Response Needs and Capabilities for Hazardous Materials Releases*, The National Academies Press, Washington, DC.
URL: *https://www.nap.edu/catalog/14502/a-guide-for-assessing-community-emergency-response-needs-and-capabilities-for-hazardous-materials-releases*

Von Stackelberg, H. (1934), *Marktform und gleichgewicht*, J. springer.

Von Stackelberg, H. (2010), *Market structure and equilibrium*, Springer Science & Business Media.

Wang, J., Kang, Y., Kwon, C. and Batta, R. (2012), 'Dual toll pricing for hazardous materials transport with linear delay', *Networks and Spatial Economics* **12**(1), 147–165.

Wiesemann, W., Tsoukalas, A., Kleniati, P.-M. and Rustem, B. (2013), 'Pessimistic bilevel optimization', *SIAM Journal on Optimization* **23**(1), 353–380.

Wood, R. K. (2010), 'Bilevel network interdiction models: Formulations and solutions', *Wiley encyclopedia of operations research and management science* .

Xu, J., Gang, J. and Lei, X. (2013), 'Hazmats transportation network design model with emergency response under complex fuzzy environment', *Mathematical Problems in Engineering* **2013**.

Zhao, J. and Ke, G. Y. (2017), 'Incorporating inventory risks in location-routing models for explosive waste management', *International Journal of Production Economics* **193**, 123–136.

Zhao, J. and Ke, G. Y. (2019), 'Optimizing emergency logistics for the offsite hazardous waste management', *Journal of Systems Science and Systems Engineering* **28**(6), 747–765.

Zhao, J. and Verter, V. (2015), 'A bi-objective model for the used oil location-routing problem', *Computers & Operations Research* **62**, 157–168.

Zheng, Y., Fang, D. and Wan, Z. (2016), 'A solution approach to the weak linear bilevel programming problems', *Optimization* **65**(7), 1437–1449.

Zheng, Y., Zhang, G., Han, J. and Lu, J. (2016), 'Pessimistic bilevel optimization model for risk-averse production-distribution planning', *Information Sciences* **372**, 677–689.

Zheng, Y., Zhu, Z. and Yuan, L. (2016), 'Partially-shared pessimistic bilevel multi-follower programming: concept, algorithm, and application', *Journal of Inequalities and Applications* **2016**(1), 1–13.

Zografos, K. G. and Androutsopoulos, K. N. (2008), 'A decision support system for integrated hazardous materials routing and emergency response decisions', *Transportation Research Part C: Emerging Technologies* **16**(6), 684–703.

Appendices

Appendix A

Bilevel Model

This appendix shows the complete formulation of our proposed bilevel model. In more details, Objective (A.1) is the pessimistic risk evaluation as indicated in Figure 3.2. Constraints (A.2) to (A.9) are the upper-level constraints given in Section 3.5.1 (i.e., Constraints (3.18) to (3.25)). On the other hand, the constraint minimizing the carriers' travelled distance (Objective (A.10)) is the same as the objective of the lower-level (Objective (3.26) in Section 3.5.2), and Constraints (A.11) to (A.13) are the constraints of the lower-level (i.e., Constraints (3.27) to (3.29) in Section 3.5.2).

$$\min_{y,v,h} \quad \max \sum_{m\in\mathcal{N}} \sum_{(i,j)\in\mathcal{A}} \sum_{c\in\mathcal{C}} R_{ij}^{c}\alpha(t_{ij}^{m})h_{ij}^{m}x_{ij}^{c} \tag{A.1}$$

$$\text{s.t.} \quad \sum_{m\in N} v^{m} \leq H \tag{A.2}$$

$$h_{ij}^{m} \leq v^{m} \qquad \forall (i,j)\in\mathcal{A}, \forall m\in\mathcal{N} \tag{A.3}$$

$$\sum_{m\in N} h_{ij}^{m} \geq x_{ij}^{c} \qquad \forall (i,j)\in\mathcal{A}, \forall c\in\mathcal{C} \tag{A.4}$$

$$\sum_{m \in N} h_{ij}^m \leq 1 \qquad \forall (i,j) \in \mathcal{A} \tag{A.5}$$

$$P(T_{ij}^m h_{ij}^m \leq T_{best}) \geq \gamma \qquad \forall (i,j) \in \mathcal{A}, \forall m \in \mathcal{N} \tag{A.6}$$

$$P(T_{ij}^m h_{ij}^m \leq T_{worst}) \geq \beta \qquad \forall (i,j) \in \mathcal{A}, \forall m \in \mathcal{N} \tag{A.7}$$

$$y_{ij} = y_{ji} \qquad \forall (i,j) \in \mathcal{A} \tag{A.8}$$

$$y_{ij}, v^m, h_{ij}^m \in \{0,1\} \qquad \forall (i,j) \in \mathcal{A}, \forall c \in \mathcal{C} \tag{A.9}$$

$$x_{ij}^c \in \arg\min_x \sum_{c \in \mathcal{C}} \sum_{(i,j) \in \mathcal{A}} \sum_{m \in \mathcal{N}} n^c l_{ij} x_{ij}^c \tag{A.10}$$

$$\text{s.t.} \qquad \sum_{i \in \mathcal{N}:(i,j) \in \mathcal{A}} x_{ij}^c - \sum_{l \in \mathcal{N}:(i,l) \in \mathcal{A}} x_{jl}^c = \begin{cases} 1, & j = o^c \\ -1, & j = d^c \\ 0, & \text{otherwise} \end{cases} \qquad \forall j \in \mathcal{N}, \forall c \in \mathcal{C} \tag{A.11}$$

$$x_{ij}^c \leq y_{ij} \qquad \forall (i,j) \in \mathcal{A}, \forall c \in \mathcal{C} \tag{A.12}$$

$$x_{ij}^c \in \{0,1\} \qquad \forall (i,j) \in \mathcal{A}, \forall c \in \mathcal{C} \tag{A.13}$$

Appendix B

Single Level Problem Linearization

SLP:

$$\min \quad \theta \tag{B.1}$$

$$\text{s.t.} \quad \sum_{m\in\mathcal{N}}\sum_{(i,j)\in\mathcal{A}}\sum_{c\in\mathcal{C}} R_{ij}^{c}\alpha(t_{ij}^{m})w_{ij}^{cm} \leq \theta \tag{B.2}$$

$$\sum_{m\in\mathcal{N}} v_m \leq H \tag{B.3}$$

$$h_{ij}^{m} \leq v^{m} \qquad \forall (i,j)\in\mathcal{A}, \forall m\in\mathcal{N} \tag{B.4}$$

$$\sum_{(i,j)\in\mathcal{A}} h_{ij}^{m} \geq y_{ij} \qquad \forall (i,j)\in\mathcal{A}, \forall c\in\mathcal{C} \tag{B.5}$$

$$\sum_{(i,j)\in\mathcal{A}} h_{ij}^{m} \leq 1 \qquad \forall (i,j)\in\mathcal{A} \tag{B.6}$$

$$P(T_{ij}^{m}h_{ij}^{m} \leq T_{best}) \geq \gamma \qquad \forall (i,j)\in\mathcal{A}, \forall m\in\mathcal{N} \tag{B.7}$$

$$P(T_{ij}^{m}h_{ij}^{m} \leq T_{worst}) \geq \beta \qquad \forall (i,j)\in\mathcal{A}, \forall m\in\mathcal{N} \tag{B.8}$$

$$y_{ij} = y_{ji} \qquad \forall (i,j)\in\mathcal{A} \tag{B.9}$$

$$\sum_{i\in\mathcal{N}:(i,j)\in\mathcal{A}} x_{ij}^{c} - \sum_{i\in\mathcal{N}:(i,j)\in\mathcal{A}} x_{ji}^{c} = \begin{cases} 1 & j = o^{c} \\ -1 & j = d^{c} \\ 0 & \text{otherwise} \end{cases} \qquad \forall j\in\mathcal{N}, \forall c\in\mathcal{C} \tag{B.10}$$

$$x_{ij}^c \leq y_{ij} \qquad \forall (i,j) \in \mathcal{A}, \forall c \in \mathcal{C} \qquad \text{(B.11)}$$

$$\pi_j^c - \pi_i^c \leq n^c l_{ij} + M(1 - y_{ij}) \qquad \forall (i,j) \in \mathcal{A}, \forall c \in \mathcal{C} \qquad \text{(B.12)}$$

$$\pi_{d^c}^c - \pi_{o^c}^c \geq \sum_{(i,j) \in \mathcal{A}} n^c l_{ij} x_{ij}^c \qquad \forall c \in \mathcal{C} \qquad \text{(B.13)}$$

$$h_{ij}^m + x_{ij}^c - w_{ij}^{cm} \leq 1 \qquad \forall (i,j) \in \mathcal{A}, \forall c \in \mathcal{C}, \forall m \in \mathcal{N} \qquad \text{(B.14)}$$

$$h_{ij}^m + x_{ij}^c \geq 2 w_{ij}^{cm} \qquad \forall (i,j) \in \mathcal{A}, \forall c \in \mathcal{C}, \forall m \in \mathcal{N} \qquad \text{(B.15)}$$

$$x_{ij}^c \in \{1,0\}, y_{ij} \in \{1,0\}, v^m \in \{1,0\}, h_{ij}^m \in \{1,0\} \qquad \text{(B.16)}$$

$$\pi^c \text{ free} \qquad \text{(B.17)}$$

$$w_{ij}^{cm} \geq 0 \qquad \text{(B.18)}$$

Appendix C

Improved Linear Model

SLPIL:

$$\min \quad \theta \tag{C.1}$$

$$\text{s.t.} \quad \sum_{m\in\mathcal{N}}\sum_{(i,j)\in\mathcal{A}}\sum_{c\in\mathcal{C}} R_{ij}^{c}\alpha(t_{ij}^{m})h_{ij}^{mc} \leq \theta \tag{C.2}$$

$$\sum_{m\in N} v^{m} \leq H \tag{C.3}$$

$$h_{ij}^{mc} \leq v^{m} \qquad \forall(i,j)\in\mathcal{A}, \forall m\in\mathcal{N}, \forall c\in\mathcal{C} \tag{C.4}$$

$$\sum_{m\in N} h_{ij}^{mc} \geq x_{ij}^{c} \qquad \forall(i,j)\in\mathcal{A}, \forall c\in\mathcal{C} \tag{C.5}$$

$$P(T_{ij}^{m}h_{ij}^{mc} \leq T_{best}) \geq \gamma \qquad \forall(i,j)\in\mathcal{A}, \forall m\in\mathcal{N}, \forall c\in\mathcal{C} \tag{C.6}$$

$$P(T_{ij}^{m}h_{ij}^{mc} \leq T_{worst}) \geq \beta \qquad \forall(i,j)\in\mathcal{A}, \forall m\in\mathcal{N}, \forall c\in\mathcal{C} \tag{C.7}$$

$$y_{ij} = y_{ji} \qquad \forall(i,j)\in\mathcal{A} \tag{C.8}$$

$$\sum_{i \in N:(i,j) \in A} x_{ij}^c - \sum_{i \in \mathcal{N}:(i,j) \in \mathcal{A}} x_{ji}^c = \begin{cases} 1 & \text{j=o(c)} \\ -1 & \text{j=d(c)} \\ 0 & \text{otherwise} \end{cases} \qquad \forall j \in \mathcal{N}, \forall c \in \mathcal{C} \tag{C.9}$$

$$x_{ij}^c \leq y_{ij} \qquad \forall (i,j) \in \mathcal{A}, \forall c \in \mathcal{C} \tag{C.10}$$

$$\pi_j^c - \pi_i^c \leq n^c l_{ij} + M(1 - y_{ij}) \qquad \forall (i,j) \in \mathcal{A}, \forall c \in \mathcal{C} \tag{C.11}$$

$$\pi_{d(c)}^c - \pi_{o(c)}^c \geq \sum_{(i,j) \in A} n^c l_{ij} x_{ij}^c \qquad \forall c \in \mathcal{C} \tag{C.12}$$

$$x_{ij}^c \in \{1,0\}, y_{ij} \in \{1,0\}, v^m \in \{1,0\}, h_{ij}^{mc} \in \{1,0\} \tag{C.13}$$

$$\pi_j^c \text{ free} \tag{C.14}$$